Bernardo José Santos de Oliveira e Silva

Assessment of Accelerometer Signals for Detection of Faint Onset during Tilt Table Tests

Thesis submitted to the University of Coimbra in compliance with the requirements for the degree of Master in Biomedical Engineering

September, 2017

· U C ·

UNIVERSIDADE DE COIMBRA

• U C •

FCTUC FACULDADE DE CIÊNCIAS
E TECNOLOGIA
UNIVERSIDADE DE COIMBRA

BERNARDO JOSÉ SANTOS DE OLIVEIRA E SILVA

Assessment of Accelerometer Signals for Detection of Faint Onset during Tilt Table Tests

Dissertação apresentada à Universidade de Coimbra para cumprimento dos requisitos necessários à obtenção do grau de Mestre em Engenharia Biomédica

Thesis submitted to the University of Coimbra in compliance with the requirements for the degree of Master in Biomedical Engineering

Supervisors:

Paulo de Carvalho, PhD

Jens Muehlsteff, PhD

Coimbra, 2017

This work was developed in collaboration with:

Centre for Informatics and Systems of the University of Coimbra

PHILIPS Research Europe

This Master Thesis has received funding from the European Union's Horizon 2020 research and innovation programme under grant agreement No 692023.

Acknowledgments

First of all, I would like to express my gratitude to the Physics Department of the University of Coimbra, for receiving me during the amazing past 5 years.

I am also thankful to the Link project (grant agreement No 692023) for the financial support, to Philips Research Eindhoven, for having allowed and supported a stay in the Netherlands with the aim of gaining new experiences, deepening and developing the thesis work, and also to the Polytechnic University of Milan, namely to Prof. Anna Bianchi for the useful contents discussed during the stay in Milan.

I am also very grateful to Prof. Paulo Carvalho and Dr. Jens Muehlsteff for their knowledge, availability demonstrated, great advices and time spent, always ready to help.

How could it not be, a special thanks to my friends from Zoo, Trianon and Baladas, who made these years even more amusing and interesting than they were meant to be.

I am also especially grateful to Ana Sofia Oliveira for the comprehension, motivation, and the encouragement given throughout the thesis development, always trying to help and contribute, always with me both in good and bad times.

Above all, I am grateful to my family, especially to my parents and sister, always being there for me, supporting and advising me in every choice that I´ve made.

Abstract

Syncope is a disorder of the autonomic regulation of postural tone. It is characterized by blood-pressure regulation failure resulting in hypoperfusion of the brain, which might lead to a transient loss of consciousness. Hence, a detection of the onset of the blood pressure decrease enables the patient to start counter-measures and avoid the faint. The damages of syncope are most of all related to falls and accidents as a consequence of the faint, having a greater impact on the elderly leading to possible fractures or bruises. In this way, it is increasingly necessary to develop a continuous blood pressure monitoring mechanism in order to anticipate and predict a syncope event.

Another public health problem that society is forcing to lead with is the cardiac arrest, claiming every year more than 400 000 American adults' lives. The duration of the resuscitation process and is a crucial factor of survival and of the sequelae that this event may cause. Manual palpation is the "golden reference" for pulse check during cardiopulmonary resuscitation, however, is an error prone procedure and often takes too long. The procedure consists of placing a finger above an artery close to the skin surface to feel pulsations. Therefore, taking into consideration the importance of the efficiency and velocity of the resuscitation process, it is extremely important to improve the mechanism for pulse assessment, not only in the case of cardiac arrest but whenever a person is unconscious with pulseless.

Accelerometer sensor (ACC), placed above the carotid artery, may be an interesting approach with potential to help to solve both problems mentioned. However, they are highly prone to movement artifacts. Therefore, in the first phase of the thesis, the challenge was to design a solution using the accelerometer to identify motion artifacts properly. A computationally simple solution was investigated to develop a noise classifier for the identification of movement artifacts in accelerometer signals acquired from the carotid. In the second phase, the aim was to do an initial investigation of using a fusion approach between accelerometer signals (acquired from the carotid) and electrocardiogram (ECG) signals to reliably infer the pulse presence and pulse absence. For that, it was developed a classifier using a cross-correlation feature derived from the ECG and the ACC signals. Posteriorly, also from the cross-correlation between both signals, was inferred the pulse arrival time (PAT) as a blood pressure surrogate feature.

Regarding the noise classifier developed during the first phase it was demonstrated that is possible to use simple features and achieve an artifact detection sensitivity and specificity higher than 90%. Concerning the second phase, for accelerometer signals with high signal-to-noise ratio (SNR) the correlation coefficient revealed to be able to discriminate phases of pulse presence versus pulse absence, registering sensitivity and specificity also higher than 90%. However, this approach appeared to be highly susceptible to contaminations for the PAT extraction, which compromises the usability of this feature as a blood pressure surrogate.

Keywords: Accelerometer, Pulse Detection, Blood Pressure Regulation, Syncope, Cardiopulmonary Resuscitation.

Resumo

A Síncope corresponde a uma desordem ao nível da regulação do tónus postural. Está associada a uma perda transitória de consciência, causada por uma hipoperfusão de sangue a nível cerebral resultante de uma insuficiência da regulação da pressão sanguínea. Assim, uma deteção precoce do início da diminuição da pressão sanguínea permite à pessoa realizar contramedidas de forma a minorar danos de um possível desmaio, ou até mesmo evitá-lo. Os danos relacionados com a síncope estão maioritariamente relacionados com quedas ou acidentes consequentes do desmaio, tendo especial impacto na população mais idosa, levando a possíveis fraturas ou contusões. Desta forma, torna-se cada vez mais importante o desenvolvimento de um mecanismo de monitorização contínua de pressão sanguínea para antecipar e prever eventos de síncope.

Um outro problema de saúde pública com o qual a sociedade é forçada a lidar são ataques de paragem cardíaca, que causam anualmente a morte de 400 000 Americanos adultos. A duração do processo de reanimação é um fator crucial de sobrevivência e de possíveis sequelas que possam surgir após o ataque. A palpação manual é o principal método para a verificação de pulso durante a ressuscitação cardiopulmonar, no entanto, é um procedimento propício a erros e muitas vezes bastante moroso. O procedimento consiste na colocação de um dedo acima de uma artéria próxima da superfície da pele de forma a sentir as pulsações. Assim, dada a importância da eficiência e rapidez do processo de reanimação, é extremamente importante melhorar o mecanismo de deteção de pulso, não só em casos de ataque cardíaco, mas sempre que um indivíduo esteja inconsciente e sem pulso.

O sensor de acelerómetro (ACC), colocado ao nível da artéria carótida, poderá ser uma abordagem interessante e com potencial para auxiliar na resolução dos problemas mencionados. No entanto, este sensor é consideravelmente suscetível a artefactos de movimento. Assim, numa primeira fase da presente tese, o desafio passou por elaborar uma solução usando o acelerómetro para a identificação de artefactos de movimento apropriadamente. Um método computacional simples foi testado para a elaboração de um classificador de ruído que permitisse a identificação de artefactos de movimento em sinais de acelerómetro adquiridos a partir da carótida. Na segunda fase, o objetivo passou por uma avaliação inicial no uso de uma abordagem baseada na fusão entre os sinais de acelerómetro e eletrocardiograma (ECG) para inferir viavelmente a presença/ausência de

pulso. Para isso, foi desenvolvido um classificador baseado em propriedades extraídas a partir da correlação-cruzada entre os sinais de ECG e ACC. Posteriormente, recorrendo também à correlação-cruzada entre os dois sinais, inferiu-se o tempo de chegada do pulso (PAT) como parâmetro de substituição da pressão sanguínea.

Relativamente ao classificador de ruído desenvolvido durante a primeira fase, foi demonstrado que, usando um modelo simples, é possível alcançar uma sensibilidade e especificidade de deteção de artefactos superiores a 90%. Quanto à segunda fase, para os sinais do acelerómetro com elevada relação sinal-ruído (SNR), o coeficiente de correlação revelou ser capaz de discriminar fases de presença e ausência de pulso, registando sensibilidade e especificidade também superiores a 90%. No entanto, essa abordagem pareceu ser altamente suscetível a contaminações para a extração de PAT, o que poderá comprometer a usabilidade deste parâmetro como substituto da pressão sanguínea.

Palavras-chave: Acelerómetro, Deteção de Pulso, Regulação da Pressão Sanguínea, Síncope, Ressuscitação Cardiopulmonar.

Contents

Acronyms

Abs. ACC	Absolute Value of the Accelerometer Signal
ACC	Accelerometer
ACC_X	Axis x of the Accelerometer Signal
ACC_Y	Axis y of the Accelerometer Signal
ACC_Z	Axis z of the Accelerometer Signal
AUC	Area Under the Curve
AV	Atrioventricular Node
BMI	Body Mass Index
BP	Blood Pressure
CPR	Cardiopulmonary Resuscitation
DBP	Diastolic Blood Pressure
ECG	Electrocardiogram
EM	Energy Mean
EV	Energy Variance
ED	Emergency Department
FSS	Feature Selection Score
HR	Heart Rate
HUTT	Head-up Tilt Table
LC	Inductive Capacitive
LED	Light-emitting Diode
LVET	Left Ventricular Ejection Time
MAP	Mean Aortic Pressure
mBP	Mean of Blood Pressure
MPA	Maximum Positive Amplitude

NMS	Neurally Mediated Syncope
PAT	Pulse Arrival Time
pBP	Pulse Blood Pressure
PEP	Pre-ejection Period
PPG	Photoplethysmogram
PR	Pulse Rate
PRV	Pulse Rate Variability
PTT	Pulse Transit Time
PVC	Premature Ventricular Contractions
PWV	Pulse Wave Velocity
RCC	Spearman's rank correlation coefficient
RI	Reflection Index
ROC	Receiver Operating Characteristic
SA	Sinoatrial Node
SBP	Systolic Blood Pressure
SEN	Sensitivity
SHE	Shannon Energy
SI	Stiffness Index
SM3	3º Statistical Moment of the Energy
SM4	4º Statistical Moment of the Energy
SNR	Signal-to-noise Ratio
SPE	Specificity
SVD	Singular Value Decomposition
TE	Teager Energy

List of Figures

List of Tables

Chapter 1

Introduction

1.1. Contextualization and Motivation

The overall goal of this dissertation is to assess the use of low-intrusive, simple and cheap accelerometer sensors in two relevant medical applications: syncope prediction and cardiopulmonary resuscitation. For this end, technical solutions for real life application scenarios are introduced and their suitability and accuracy assessed.

Syncope refers to a sudden and transient loss of consciousness with complete spontaneous recovery, resulting from a temporary blood hypoperfusion to the brain [1], [2]. Given that most syncope events could have been prevented, the impact that it has on the society, especially on the elderly population, and on health costs is huge. In Europe, 0.9 to 1.2% of emergency department (ED) visits correspond to events related to syncope, and in the United States of America they account for 3% of ED, representing 1 to 6% of admissions of all hospitals in general [3], [4]. The incidence of syncope events is higher in the elderly, with a growing costs associated with increasing age [5], mainly due to the falls caused by fainting, leading to possible fractures or bruises. As an example, the United Kingdom government has expenses of over £ 1 billion per year, just with falls in elderly [6]. Thus, with a greater incidence in individuals over 45 years old, in an aging society, it is expected an increase on the present costs related to syncope, in the absence of countermeasures [4], [7]. In this way, it is increasingly necessary to develop a continuous monitoring mechanism in order to anticipate and predict a syncope event, so that the person can take countermeasures, such simple as lying or sitting down, minimizing possible injuries.

Another public health problem that society is forcing to deal with is cardiac arrest. Cardiac arrest claims every year the lives of more than 400 000 American adults and represents a major cause of cardiovascular death [8]. The duration of the resuscitation process is a crucial factor of survival and of the sequelae that this event may cause, and it is defined as the set of two distinct intervals: the interval from the attack to the initiation of the cardiopulmonary resuscitation (CPR) and the interval from the beginning of the

CPR until a spontaneous circulation is restored or the resuscitation termination. It is demonstrated that a strong correlation is observed between the first interval of the resuscitation process and the survival status, with a survival rate lower than 1% if the duration of this interval exceeds 14 minutes. Thus, the longer the reaction period takes, the lower the survival status and the worse the sequelae suffered after the cardiac arrest event [9]. Therefore, it is extremely important to improve the reaction period and the efficiency of the resuscitation process, not only in the case of cardiac arrest, but whenever a person is unconscious without pulse. Manual pulse palpation is the most common procedure to assess pulse in unconscious patients. The procedure consists of placing a finger above an artery close to the skin surface such as the carotid, femoral or radial artery and to feel the pulsations. This is an error prone procedure and often takes too long. However, it is still the "golden reference" for pulse check during CPR [10]–[15]. Consequently, a reliable and automatic pulse detection technique should also be a priority in order to improve the responsiveness and the efficiency of the resuscitation process.

An interesting and promising sensing modality for both problems is accelerometer (ACC) sensor. They are low cost, low power, small and inexpensive sensors but with high sensitivity [10], [16]. Therefore, the aim of this thesis is to assess whether the accelerometer sensor might be used as an information source for the development of reliable and viable mechanisms to support resuscitation techniques such as CPR and prediction of syncope events.

1.2. Thesis Structure

The current document is divided into the following chapters:

- Chapter 2 – Physiological and Measurement Background - where it is described all the physiological background required for understanding syncope and CPR.
- Chapter 3 – State of the Art - where previous work developed related to syncope prediction and cardiopulmonary resuscitation is presented and assessed with respect to limitations and challenges.
- Chapter 4 – Artifact detection in Accelerometer Signals from the Carotid - corresponds to the first stage of the thesis, where a noise classifier for the

Accelerometer signals, based on simple energy features, is developed. It is tuned for the detection of high-frequency or high-intensity interferences.

- Chapter 5 – Robust Carotid Pulse Detection Using Accelerometry and Electrocardiography and Pulse Arrival Time Extraction - reports the second and last stage of the thesis, where after a selection of the clean segments of the signal, there is also a selection of the segments with/without pulse presence and subsequent pulse arrival time extraction.
- Chapter 6 – Conclusion and Future work - the final conclusions and the potential evolutions are described.

1.3. Contributions and Publications

This thesis has two main contributions:

- A noise classifier algorithm for the accelerometer signals was developed and is described in Chapter 4. It has culminated with the elaboration of a scientific article entitled "Artifact detection in Accelerometer Signals acquired from the Carotid" and presented at the 39th Annual International Conference of the Engineering in Medicine and Biology Society (EMBC' 17) of the Institute for Electrical and Electronics Engineers (IEEE), Seoul, South Korea, 2017 (see Appendix A).
- A pulse presence detection algorithm with posteriorly Systolic Blood Pressure surrogate feature inference was introduced. It is described in the Chapter 5. Part of this work was described in another scientific article entitled "Robust Carotid Pulse Detection Using Accelerometry ad Electrocardiography". This paper was submitted and accepted to be presented at the 3rd International Forum on Research and Technologies for Society Industry (RSTI 2017) of the Institute for Electrical and Electronics Engineers (IEEE), in Modena, Italy, 2017 (see Appendix B).

Chapter 2

Physiological and Measurement Background

In this chapter, all the concepts concerning the physiological and measurement background necessary for a correct understanding and elaboration of the research work, are presented.

2.1. Cardiovascular System

The cardiovascular system is one of the most important systems in the human body, from which all other systems depend directly. It is responsible for the transportation of oxygen, nutrients, hormones and waste products from the cells metabolism. It also has a very active role on the human body temperature regulation and on the immune response [17].

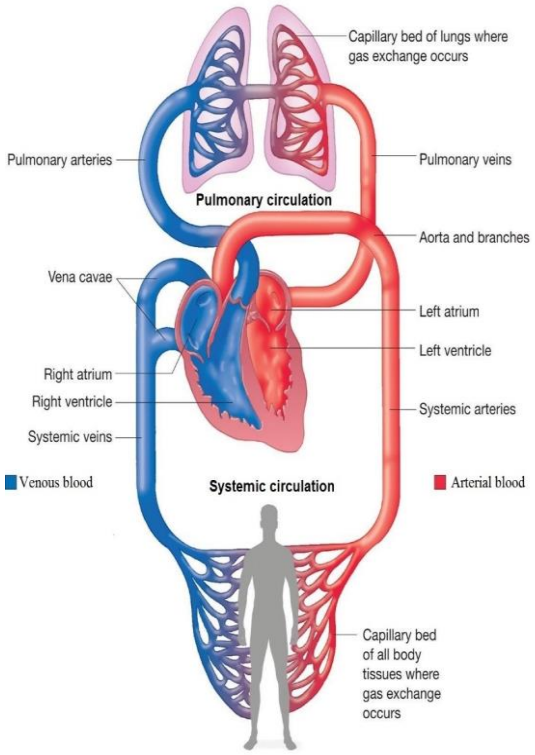

Figure 1 - Schematic representation of the cardiovascular system and blood circulation [19].

The cardiovascular system is composed by two components: the heart that is responsible for pumping the blood allowing capillary irrigation, and the blood vessels that define the closed system for the blood to flow. In a normal situation, the heart's pumping leads to pressure gradients that force the blood to circulate in a unidirectional way. This cycle is divided in two interconnected different circulations: the pulmonary circulation and the systemic circulation (see Figure 1) [17]. In the pulmonary circulation, the blood is pumped from the right ventricle to the lungs for gas exchange. Here, the deoxygenated blood releases carbon dioxide and receives oxygen, returning to the heart through the left atria. In this circulation, the blood passes from venous blood (deoxygenate blood) to arterial blood (oxygenate blood). Simultaneously, on the systemic circulation, the arterial blood is pumped from the left ventricle to all the body tissues. Here it releases oxygen and receives carbon dioxide, as a result from the cells metabolism. The blood passes to venous blood and returns to the heart through the right atria [18].

An important fact to refer is that the vessels responsible for the transportation of the blood from the heart are the arteries. The veins are responsible to transport the blood to the heart again [18].

2.1.1. The Heart

The heart is a muscular organ constituted by four separated chambers. Two atria, which are the superior receiving chambers and two ventricles, the inferior pumping chambers. Both ventricles are separated by a septum that prevents the mixing of venous blood with arterial blood, allowing to have the two types of circulation, and divides the heart in a right and left side (one ventricle and one atria on each side). On the right side of the heart, only venous blood does flow. The atria receives the blood from the Systemic circulation, and posteriorly the ventricle pumps it to the lungs. On the left side circulation is restricted to arterial blood. The atria receives the blood from the lungs and posteriorly the ventricle pumps it to the entire body. Consequently, the left ventricle is more robust than the right ventricle, because it has to pump the blood for the entire body, which requires more effort than just to pump the blood to the lungs [18].

It is also important to mention that the unidirectional flow is only possible due to the presence of valves (mitral and tricuspid valves) between the atria and the ventricles. It prevents the blood returning to the atria when it is pumped (see Figure 2) [17].

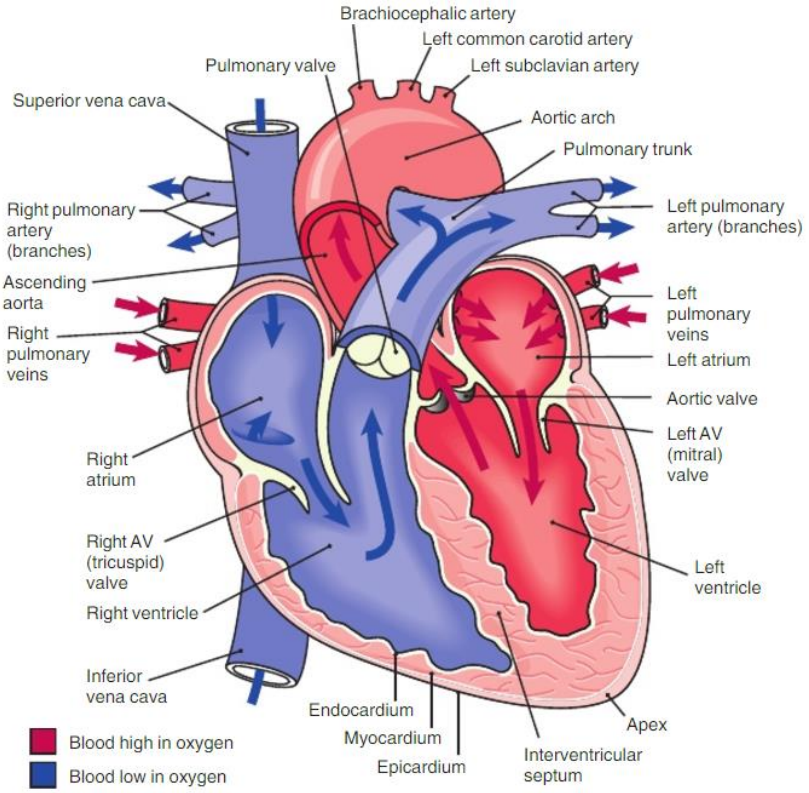

Figure 2 – Heart's anatomy and circulatory flow represented by the blue a red arrows [20].

Behind all the movements of contraction and relaxation of the heart and its chambers is an efficient system of electrical stimulus. The conduction system of the heart regulates the contraction of the ventricles and atria in order to have the same contraction rates. This enables an efficient and functional blood circulation. Therefore, the heart beat is coordinated by nodal tissue. It has both muscular and nervous characteristics and is located in two different regions of the heart. On the right atria it is the sinoatrial node (SA), responsible for the initiation of the heartbeat and contraction of the atria. The atrioventricular node (AV) is located between the right atrium and right ventricle and causes the delay of the impulse transport, allowing the atria to finish their contraction before the ventricles start their contraction [17].

The cardiac cycle corresponds to all the events that occur during one heartbeat. Despite each half of the heart being responsible for different blood circulation, they have a close interaction. Both atria contract together, releasing the blood to the ventricles that also contract together, pumping the blood out of the heart. Thus, the cardiac cycle is the successive contractions (systole) and relaxation (diastole) movements that enables an effective circulation of the blood through the heart (see Figure 3) [17].

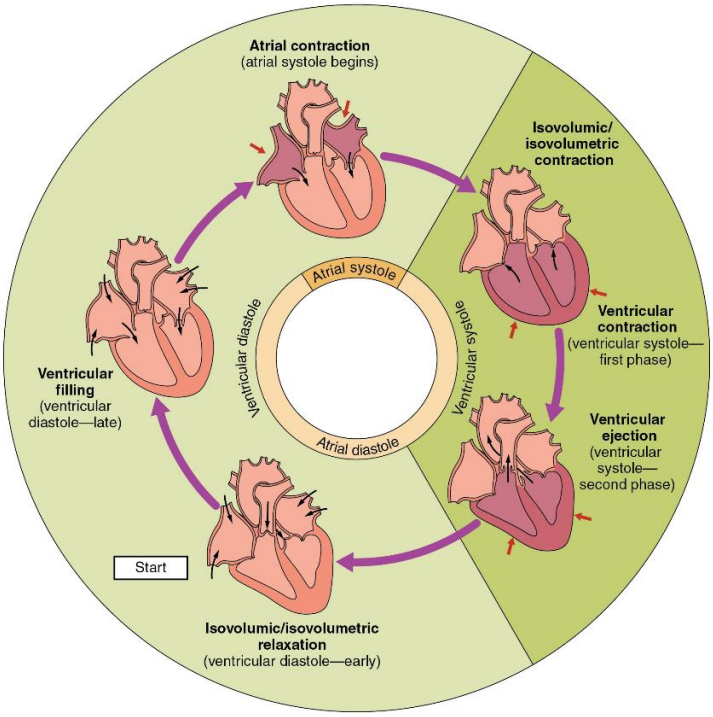

Figure 3 – Cardiac Cycle. Adapted from [21].

2.2. Blood Pressure Regulation

The blood circulation is based on a pressure gradient along the vessels caused by the pumping of blood by the heart, flowing from regions of higher pressure to region of lower pressure (the greater the pressure difference, the greater the blood flow). The pressure that the blood makes against a blood vessels wall is considered the Blood pressure (BP) [18].

The alternation of the heartbeat between systole and diastole, causes fluctuations on the BP characteristics and properties in the arterial system [17]. Thus, the arterial pressure (BP in the arteries) is pulsatile, oscillating between systolic blood pressure (SBP – pressure in the artery after a left ventricle contraction) and diastolic blood pressure (DBP – pressure in the artery before the left ventricle contraction) as is illustrated in Figure 4. Between successive ejections, in the systemic circulation the BP decays from 120 mmHg (SBP) to approximately 80 mmHg (DBP), while in the pulmonary circulation the BP decays from 25 mmHg to 10 mmHg [22].

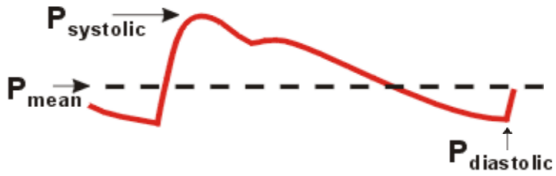

Figure 4 – The aortic blood pressure curve. Adapted from [23].

As is depicted in Figure 5, as the blood moves away from the left ventricle during the systemic circulation, its pressure decreases. This decrease of pressure is very important for capillary exchanges to be successful. The BP reaches the lowest level before the blood flows into the right ventricle [18].

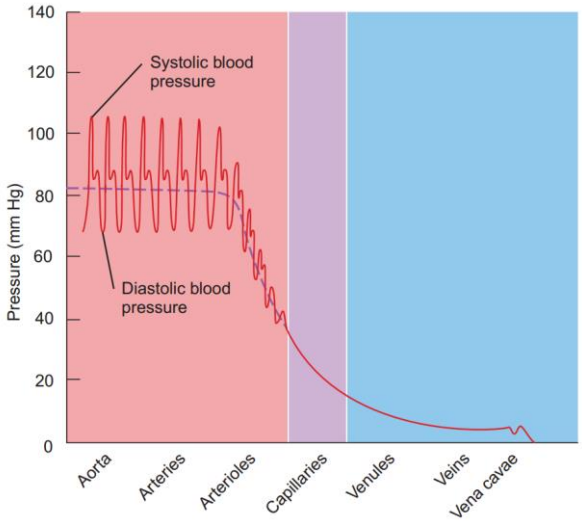

Figure 5 – Blood pressure evolution during the systemic circulation [18].

There are several physiological factors that influence the arterial blood pressure. The heart rate, the amount of blood ejected from the heart (more volume ejected leads to higher BP), the peripheral resistance (the friction between the walls of the vessel and the blood – the greater the resistance of the vessel, the greater the BP), the venous return (the blood volume that flows back to the heart through the systemic veins), are examples of those physiological factors [17], [18]. Besides these, the blood properties, as viscosity, also influence the BP.

In order for there to be a constant balance between the needs of the body according to the different conditions to which it is subjected, there must be an effective and efficient BP control. Physical activity situations, for example, require a more optimized transport of oxygen to the cells. Through variation on the heart rate, vasodilatation or vasoconstriction, etc., the BP regulation can be made by a neural or hormonal control [17], [18].

2.3. Carotid Artery

As is illustrated in Figure 6, there are three major arteries that branch out of the aortic arch: the left subclavian artery, the brachiocephalic artery and the left common carotid artery. The brachiocephalic artery posteriorly divides into the right subclavian artery and the right common carotid [17]. Each carotid ramifies into the internal and external sub-carotid. The carotid arteries are responsible for the supply of blood to the brain, face, eyes and also the neck [18]. Consequently, any injury on these arteries can lead to a very damaging situation, such as stroke.

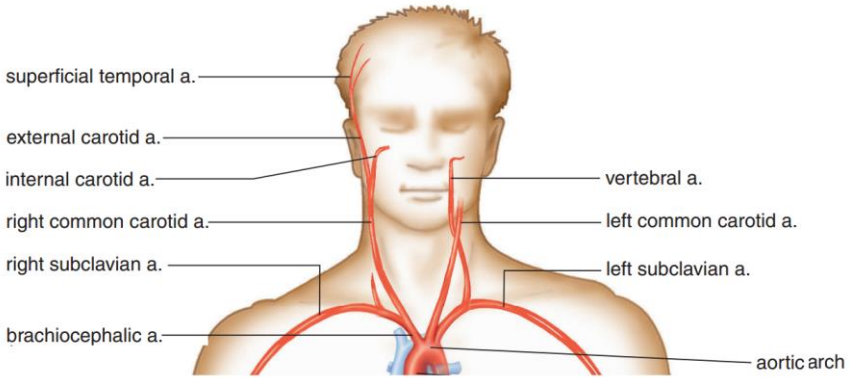

Figure 6 – Some of the major arteries form the body. Adapted from [17].

The central location, the easy access, the large diameter of the carotid artery and the fact that is relatively close to the skin surface, makes this artery a prominent site to assess the presence and the strength of a person's pulse [16].

2.4. Syncope

Syncope, or fainting, is considered as a sudden, temporary loss of consciousness, followed by a spontaneous recovery, due to cerebral hyporperfusion [18], [24]. In some forms of syncope, symptoms such as nausea, weakness, light-headedness, sweating or visual disturbances, may be a precursor, warning that a syncope event is about to occur. However, it is very usual that it happens without any detectable precursor, being, consequently, a cause of many falls or other accidents. An estimation of the duration of this spontaneous episodes is also regularly inaccurately obtained, which makes it difficult for others to know how they can manage the situation. Nevertheless, the syncope recovery is usually with an almost immediate restoration of appropriate behavior and orientation

[2]. Additionally, it is important to notice that the consequences of a syncope episode, are different from person to person. In the elderly, the risk of serious injuries induced by falls is higher than in young people.

Despite the different types of syncope, there is one common cause to all of them: a fall in systemic blood pressure accompanied by a decrease global cerebral blood flow, is in the basis for syncope. A cessation of just 6-8 seconds of blood flow into the brain is enough to cause a loss of consciousness, namely when the systolic blood pressure decreases to 60 mmHg or lower a syncope episode can occur [2]. Therefore, a physiological reflex causing bradycardia, cardiovascular problems as arrhythmias or structural disease including pulmonary embolism or hypertension and inadequate venous return, due to volume depletion or venous pooling, compose the main causes that define the three different types of syncope respectively: neutrally mediated syncope; cardiac syncope; syncope due to orthostatic hypotension [2], [24].

2.4.1. Neurally Mediated Syncope

Neurally mediated syncope (NMS) or reflex syncope is the most common type of syncope and it refers to situations when the cardiovascular effector mechanisms that are usually useful in the blood circulation control become overactive and intermittently inappropriate in response to abrupt stimulus as post exercise condition or emotional stress. This can result in vasodilatation and/or bradycardia, which will lead to a fall in arterial blood pressure and decrease in cerebral perfusion, culminating in fainting [2], [24].

Reflex syncope may be classified based on the efferent pathway or in the afferent pathway. On the efferent point of view, it can be classified as vasodepressor if the cause is the loss of the upright vasoconstrictor tone, predominating hypotension, as cardioinhibitory if bradycardia or asystole predominates, or as mixed if both mechanisms are present [2]. The afferent classification is based on which trigger caused the syncope´s event. Depending on the person, the triggering situations vary considerably. Thus, in an afferent point of view it can be classified as: vasovagal syncope, if it is preceded by prodromal symptoms of autonomic activation (sweating, nausea, pallor) and is mediated by orthostatic stress or emotion; situational syncope, is mainly caused by specifics circumstances as post exercise, gastrointestinal stimulation, micturition, etc.; Carotid

sinus syncope, it is a spontaneous rare form caused by mechanical manipulation of the carotid sinuses; atypical form, describes the situations in which the trigger is uncertain or even apparently absent [2].

2.4.2. Cardiac Syncope

The cardiac syncope can be caused by arrhythmias and structural cardiac disease. In both cases the syncope occurs due to a decrease in cardiac output (volume ejected from a ventricle in one minute [18]) [24]. Consequently, a decrease of it, leads to a decrease in BP and to a decrease in cerebral blood perfusion level.

In this kind of syncope, the loss of consciousness, usually occurs between 20-120 seconds later than the onset of the arrhythmia. Therefore, the BP drops slower, allowing the person to have enough time to proceed in order to minimize consequences such as injuries due to falls [24].

In the case where a structural disease is the cause of a syncope event, the circulatory demands outweighs the heart's capability to increase its output. Accordingly, when the cardiac output is not enough to suppress the needs of the body, the cerebral blood perfusion is compromised, leading to the occurrence of syncope [2].

2.4.3. Syncope due to Orthostatic Hypotension

The orthostatic hypotension is defined as an unnatural decrease in systolic blood pressure upon standing. Unlike neutrally mediated syncope, in autonomic failure the efferent activity is chronically impaired which mean that the vasoconstriction defective. As was mentioned, despite in a pathophysiological point of view NMS and autonomic failure being different, the symptoms of both are very similar, making it quite difficult to differential diagnosis [2].

Three successive stages characterize the evolution of this kind of syncope: the pre-syncope phase, the loss of consciousness and the post-syncope phase. The pre-syncope phase, is the phase before syncope, and at this stage the person starts to feel symptoms such as nausea, weakness and abdominal discomfort, and it may last 30 seconds. This might provide enough time for the person to initiate counter measure in order to revert the situation and to avoid possible injuries. The second phase is when the person loses

consciousness for a time between 5 and 20 seconds. Finally, the post-syncope phase, corresponds to the person's recovery, still feeling some discomfort [2].

2.5. Cardiopulmonary Resuscitation

In a situation where a resuscitation is needed, the efficiency and responsiveness of the resuscitation process can be decisive in the sequelae that may arise, or may even be the difference between life and death [25]. Therefore, any second matters. The cardiopulmonary resuscitation is a process that keeps the circulatory flow and oxygenation during cardiac arrest, through the execution of chest compressions and artificial ventilation. The CPR should be performed immediately on any person unconscious without pulse [25].

During cardiac arrest, the chest compressions allow the blood circulation by two different mechanisms: the cardiac pump and the thoracic pump. The cardiac pump occurs when the chest compressions squeezes the cardiac ventricles between the sternum and the spine. The blood flows through the aortic and pulmonic valves with a functional mitral and tricuspid valves. On the other hand, on the thoracic pump mechanism the chest compression causes a global rise in intrathoracic pressure that forces the blood to flow from the pulmonary vessels, through the heart and into the periphery. In this case, during the chest compression both mitral and aortic valves are open [26].

2.6. Contribution for the Accelerometer signal on the Carotid Artery

An accelerometer is a sensor that measures the acceleration experienced by the sensor and, consequently, the acceleration of anything to which the sensor is attached to [27]. Therefore, in the context of this thesis, attaching the sensor to the neck, the primary signal of interest to detect is the momentum changes at the skin surface provoked by dilatation of the underlying carotid artery [28]. The ejection of blood by the heart generates a pulse wave that when crossing the carotid artery, causes a variation of its diameter.

As described previously, the accelerometer sensor is highly sensitive, consequently any kind of movement that affects the sensor will have repercussions on the detected signal. Thus, the signal measured from the accelerometer consists of three different components: a gravitational, a movement and noise [29].

The gravitational component is visible as the offset of one or more sensor axes during static conditions or steady state non-rotational movement. It allows to detect the orientation of the sensor relative to the vertical plane [29], being useful to compare the changes of position of the patient with the changes of the signal's morphology.

Regarding the movement component, there are three different sources. The first one is, as mentioned and explained above, due to the dilatation of the carotid artery. This is the primary signal of interest. The other two are due to respiratory movements and ballistocardiogram [30], [31]. The movement of the thorax caused by the respiratory movements, induces vibrations on the body that can affect the ACC, and consequently be detected by the sensor [31]. Concerning the ballistocardiogram, it corresponds to the reaction (displacement, velocity or acceleration) of the body generated by the heart when it ejects blood at each cardiac cycle. Therefore, it is associated to all kind of movements of the blood inside the heart or in the arteries and the movement of heart itself [30]. It corresponds to the global body momentum changes due to the pumping of the heart [28]. Consequently, this reaction of the body interferes with the accelerometer, affecting the signal.

The noise component, is any kind of movement that may interfere with the signal besides those described previously, as arms movements, rotation of the neck, swallowing, talking, etc.

2.7. Conclusion

In this chapter it was introduced an overview of the main physiological background required to understand the work developed in this thesis. This chapter also introduced basic information regarding syncope events, their relevance and their physiological implications, as well as the cardiopulmonary resuscitation process and the types of signal to expect during the extraction of an ACC sensor from the human body.

Chapter 3

State of the Art

This chapter seeks to contextualize and to show the state of the most recent/relevant developments and studies related with the area of interest of the present thesis. Therefore, different approaches for blood pressure assessment, syncope prediction and pulse assessment during cardiopulmonary resuscitation are reviewed and discussed. A brief description of devices used to capture information for these applications is also introduced.

In this way, it aims to clarify the challenges that this work faced and the contributions to overcome the gaps of current state of the art approaches in the context of pulse assessment during CPR and syncope prediction.

3.1. Photoplethysmogram and Electrocardiogram

The photoplethysmogram (PPG) signal is obtained by an optical device that based on light intensity variation estimates the pulse pressure wave, represented in Figure 7, in the microvascular bed of tissues of a specific region of the body. It is formed by two waves: the systolic and the diastolic wave. It uses a source of light, typically Light-emitting diode (LED), and a photodetector [32].

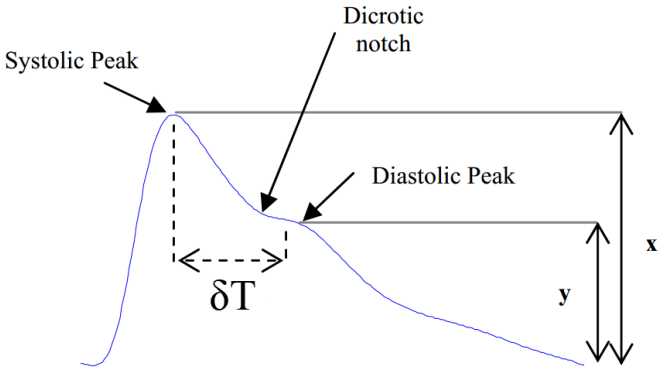

Figure 7 - PPG signal with its characteristic parameters represented. x: systolic peak amplitude. y: diastolic peak amplitude. Adapted from [33].

Despite its apparently simplicity (see Figure 7), PPG provides complex information, not just about the site where the measure is taken (usually on the finger tips), but also about heart and vessels dynamics [32]. Thus, is recurrently used in literature, not just for pulse assessment, but also for BP monitoring.

Therefore, there are many different features related to cardiovascular phenomena that can be extracted from PPG, such as:

- Pulse rate – PR – number of heartbeats per unit of time. It is measured using the time difference between the same point of two consecutive pulses [32].
- Reflection index – RI – ratio between the amplitude of the diastolic peak (y) and the systolic peak (x). It is associated with the stiffness of the small arteries [32].

$$RI = \frac{y}{x} \tag{1}$$

- Stiffness index – SI – ratio between the subject´s height and the time difference between the systolic and diastolic waves (δT) [33].

$$SI = \frac{H}{\delta T} \tag{2}$$

- Left Ventricular Ejection Time – LVET – period that takes for the blood to be ejected from the left ventricle (see Figure 8) [32].

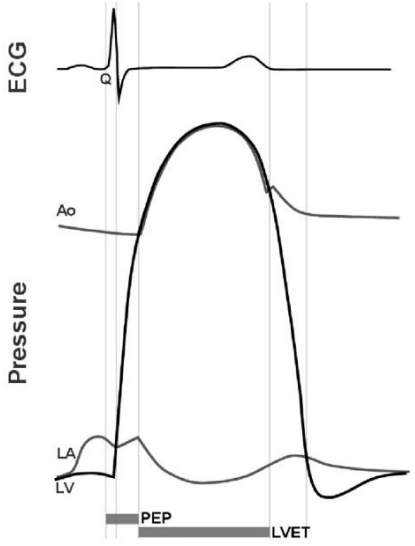

Figure 8 - Representation of LVET and PEP (Pre-ejection period). LA – Left atrium; LV – Left Ventricle; AO – Aorta. Adapted from [34].

The Electrocardiogram (ECG) is a recording of the action potentials that propagate through the heart during the cardiac cycle. It consists of a set of waves. The P wave, the complex QRS and a T wave (see Figure 9). The P wave is referent to the atrial systole, the QRS complex is referent to the depolarization of the ventricles, signalizing that they are going to be in systole. Finally, the T wave represents the ventricles repolarization, signalizing their diastole [17], [18]. From the ECC signal several useful diagnostic and prognostic information might be extracted such as the instantaneous heart rate (HR) and arrhythmic state of the heart. The ECG might be combined with other signals in order to assess relevant cardiac function as well as hemodynamic variables such as the pre-ejection period (PEP) and the pulse transit time (PTT) interval.

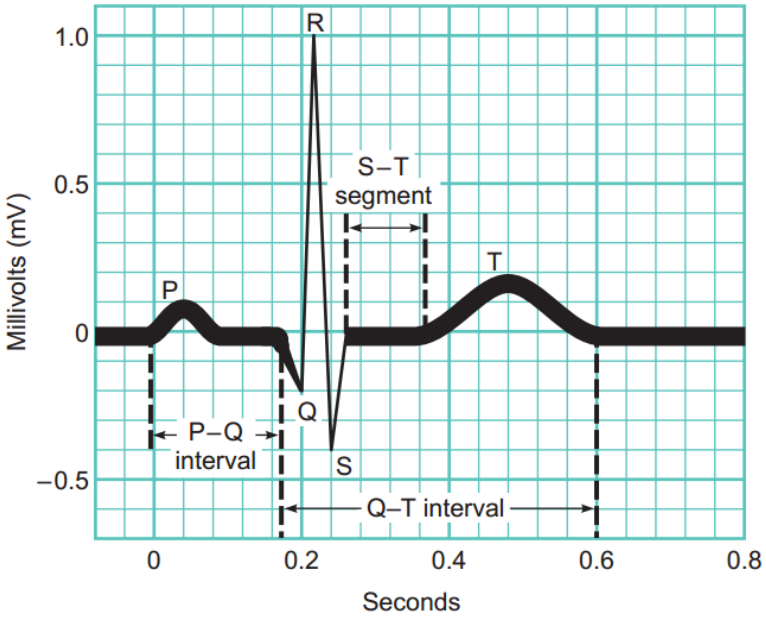

Figure 9 - Representation of an ECG and its reference points [18].

3.2. Blood Pressure Assessment

The continuous monitoring of BP has been a constant focus problem in the literature. Two examples of continuous BP measurement methods are the volume-clamp method and the arterial tonometry approach. They monitor the BP pressure continuously, based on the applanation of the radial artery to measure the pressure transmitted to the skin or based on the pressure necessary to maintain a constant vascular volume (clamp method) on the finger cuffs. In the case of the volume-clamp method, it has been already translated into commercial devices, although it has an inherent limitation. Given that it is based on the counter-pressure measurement made against the fingers in order to keep the vascular

volume constant (the higher the pressure inside the artery, the higher the counter-pressure), in long-term it will induce disturbances in the finger´s blood circulation, making it unsuitable for prolonged applications. Regarding the arterial tonometry method, it is highly susceptible to movement contaminations, restricting its application to controlled environments [35].

The complexity, cost, and the sensitivity to artifacts of current commercial wearable devices for monitoring the BP [36], leads to an investigation more centralized into BP surrogate features. An admittedly promising alternative is the pulse wave velocity (PWV) [37]. In this way, the correlation between PWV and BP can be done using the Moens-Korteweg model or using the Bramwell-Hill [35].

The Moens-Korteweg equation relates the pulse wave velocity with the elastic modulus of a thin walled, distensible, fluid-filled tube in which it is induced, and is given by:

$$PWV = \sqrt{\frac{Eh}{2r\rho}} \tag{3}$$

where E is the elastic modulus of the arterial wall, h is the wall thickness, ρ the density of the blood in an artery section and r is the vessel radius. It is expected that the main variation come from E. Posteriorly, Hughes established the connection between BP and PWV using:

$$E = E_0 e^{\gamma P} \tag{4}$$

where $E_0 = 667 \pm 382$ mmHg for the descending thoracic aorta, $\gamma \approx 0.017$ mmHg-1 and $P = P_S + K(P_S + P_d)$ corresponds to the mean aortic pressure (MAP), where P_S and P_D are the systolic and diastolic blood pressure, respectively [35], [37].

The Bramwell-Hill equation, which was derived from the previous model, relates the pressure wave velocity with the vessel compliance or distensibility. It is given by:

$$PWV = \sqrt{\frac{VdP}{\rho dV}} \tag{5}$$

with ρ being the density of the blood and V being the aortic volume at pressure P [35]. Shaltis et al. [38] by modeling with a sigmoidal curve the pressure-volume relationship, proposed the following equation:

$$V = \frac{a}{1 + e^{-bP}} \tag{6}$$

where *a* and *b* are fitting parameters [37]. Rearranging the equations (5) and (6), with Taylor expansions, it is observed that:

$$PWV = \sqrt{\frac{1 + e^{-bP}}{\rho b}} \approx \frac{1}{\sqrt{\rho b}} \frac{\sqrt{2}}{1 - \frac{bP}{4}} \equiv \frac{1}{cP - \frac{c}{4}} \tag{7}$$

with *c* as a constant determined by experimental data fitting [37].

In practice, the PWV is usually assessed recurring to the Pulse Transit Time by: $PWV = \frac{L}{PTT}$, where *L* is the distance that the pulse wave travels. PTT is defined as the time that it takes to go through that distance [35].

In this way, for the measurement of PTT, the pulse wave has to be recorded in two different locations. Typically, it is measured using the time difference between the R-peak of the ECG and the beginning of the pulse wave registered by a PPG at a peripheral site. However, this measurement is just an approximation to PTT, being frequently designated by Pulse Arrival Time (PAT). PAT consists on the sum of PEP and PTT (PAT=PEP+PTT). It is frequently used as BP surrogate instead of PTT, once it contains PEP, which is highly correlated to BP, and can be more accurately measured [35], [37].

3.3. Syncope Prediction

The syncope prediction has been a recurring theme in the literature during the last decade, largely due to the impact that it has on society, particularly in the elderly population. Although the proposed prediction approaches differ in purpose, methods or techniques applied, most of them are based on the use of the head-up tilt table (HUTT) test [37]. This test consists of lying the patient on a bed that is submitted to different tilt angles. While this occurs there is a continuous monitoring of BP, of the electrical impulses of the heart and of the oxygen level [39]. This test aims to induce fainting so that the variations of monitored properties can be analyzed and used to predict syncope in a real (not induced) situation. In case where no syncope occurs during the test, it is administered sublingually nitro-glycerin in order to trigger a hemodynamic response [16], [28].

This type of test is highly intrusive, requires specialized personnel and does not allow for real-time assessment of impending syncope episode. Therefore, a significant research effort is observed in order to develop suitable approaches to predict impending syncope episodes in real-time. Virag et al.[40], proposed a method for syncope prediction, based on the continuous analysis of BP and HR (measured from the RR intervals of ECG) changes (see Figure 9). It consists on the assessment of a cumulative risk generated by the normalized HR and SBP trends and their variability represented by low frequency power, for further comparison with a predetermined syncope risk threshold. The algorithm was tested using 1155 patients, with a sensitivity (SEN) of 95% and specificity (SPE) of 93%. The prediction time had an average of 128 ± 216 seconds. Mereu et al. approach [41] is also based on BP and HR, although the features used were different. It was assessed the ability of HR, SBP, DBP, mean of BP (mBP), pulse BP (pBP), the ratio between HR and SBP and the first derivative of the ratios HR/SBP, HR/DBP, HR/mBP and HR/pBP, as possible predictors of syncope during tilt test. The algorithm was designed for clinical facilities in order to improve patient care. The study was performed in 145 patients achieving a SEN of 86.2%, a SPE of 89.1% and a prediction time of 44.1±6.6 seconds. Both methods rely on continuous monitoring of BP which has currently several challenges and cannot be applied 24/7 [1]. The devices are expensive, complex, heavy and require a continuous recalibration and trained personal to operate [36]. Consequently, they are suited for short period of operation in hospital contexts, and are less applicable for uncontrolled environments such as home care scenarios [1]. Given this, more recent literature has been focused on techniques for a reliable estimation of BP through other features, commonly using the PPG and ECG. One example of these approaches is the one introduced by Muehlsteff et al. [42]. It is a threshold-based approach for syncope prediction using PAT from joint analysis of ECG and PPG as a BP surrogate feature. Several PAT values were extracted using different PPG reference points, i.e., the onset of the pulse, 20%, 50%, 80% of systolic peak amplitude, and the systolic peak. The detection of syncope onset was based on tracking of relative changes of PAT. The best performance was associated to the PAT extracted between R-peak and 50% of the amplitude of systolic peak, with a SEN of 90.5%, a SPE of 83% and an average of prediction time of 82 ± 78 seconds using a database collected from 44 patients.

A different approach was introduced by Couceiro et al. [43]. It achieved a better performance than the previous one, with SEN of 95.2%, SPE of 95.4% and a prediction

time of 116 ± 155.5 seconds using also the database collected from 44 patients. The algorithm applied a threshold-based classifier that uses a Minkowski distance metric. The most appropriate features for the prediction of syncope were selected, based on a feature selection score (FSS) metric. The features normalized that fed the classifier were derived from the HR (extracted from ECG), PAT (considered as time difference between ECG R-peak and 80% of the PPG systolic amplitude), LVET, SI and RI extracted from a joint between ECG and PPG. Additionally, in [44] Couceiro et al. also proposed an analysis of the variability of HR indexes as a new parameter to add to the algorithm aforementioned in [43]. This approach has resulted on the improvement of the performance with a SEN of 93.3%, SPE of 100% and a prediction time of 56.1 ± 36.8seconds.

More recently, Pinheiro in [32], introduced a fully PPG-based algorithm for syncope prediction applied in 44 patients. The method was based on a threshold classification model that uses the Minkowski distance metric. The method was based on features extracted from the following parameters: PR, extracted as a difference between characteristics points of PPG pulse, LVET, SI, RI, several pulse rate variability (PRV) indexes, second derivative of the PPG, the systolic rise of the PPG pulse wave and the information dynamics of data [32]. From these parameters, a total of 92 different features were extracted and assessed according to a ranking based on a features selection score metric. Posteriorly, different algorithms setups were assessed, and the performance of the highlighted setup was a SEN of 100 %, a SPE of 85% and a prediction time of 243 ± 226.9 seconds.

Although the aforementioned approaches have achieved good performance, PPG has some shortcomings. Since PPG is placed, for signal measurement, on a peripheral site, it is sensitive to hydrostatic effects and it is affected by vasomotion which can compromise the peripheral pulsatile blood flow, compromising the accuracy of the device. Additionally, also because of its location, the sensor can be inconvenient for the patient to carry out their daily activities, being also very susceptible to movement artifacts [16], [28], [45]. Therefore, a potential alternative technique that has been studied, is based on the utilization of an ACC sensor placed on the skin surface of the neck, above the carotid artery. As has already been mentioned in the previous chapter, due to its central location and due to the fact that the carotid artery is a prominent location for the extraction of pulse reference, it is a natural choice for the placement of ACC sensor in order to capture information sources for syncope management [46]. Muehlsteff et al. [28] developed a

physical model that simulates the arterial dilation signals acquired from an ACC sensor located on the skin surface above the carotid artery. The model results were compared with ACC measurements during a HUTT test, using the maximum positive amplitude (MPA) of each pulse of both signals. It was obtained a Person-correlation coefficient of 0.83. Besides this, in order to monitor the BP, it was tested MPA divided by HR^2 as a BP surrogate feature, demonstrating a Person-correlation coefficient of -0.8. This shows the potential of ACC sensor to extract a BP surrogate feature, although the motion artifacts may compromise its extraction. The model starts by calculating the arterial pressure variation, induced by a passing wave, to estimate the area change of the vessel. From this, it calculates the time course of the artery radius and consequently the ACC simulated signal is obtained through the second derivative of the radius calculation. It has as input parameters the age, gender, externally applied contact pressure, HR, pulse pressure and SBP.

Thus, although the ACC has been the target of some approaches for the extraction of signals from the human body (see e.g. [46], [47]) and these can sometimes be useful for syncope prediction, the use of this sensor directly to help solving this problem has not been fully and extensively explored.

3.4. Cardiopulmonary Resuscitation

Cardiopulmonary resuscitation has also been the subject of constant studies in the literature, since its efficiency and speed reveal a great importance in the sequelea that may arise from a cardiac arrest or loss of consciousness with pulseless. The way it is done can even be a deciding factor between life and death [9].

The “golden reference” for the assessment of the pulse presence during CPR is still manual palpation. However, it is error prone and often takes too long [10]. Hence, an optimization of the resuscitation process can start from a more efficient monitoring of pulse presence.

According to what was found in literature, the only solution for pulse assessment that is currently commercially available to support aiders is the CPR Check (CardiAid, California, United Sates of America). It uses a resonant non-linear inductive-capacitive (LC) sensor to track pulse and respiration [10]. A LC-oscillating circuit allows the

acquisition of electrical signals originated by variation of distance between the sensor and region of interest, in this case the skin. Therefore, the pulse wave and respiration cause variation in the surface of the tissue that affect the resonance circuit and, consequently, generate a signal that allows the monitoring [48].

Wijshoff et al. [49] investigated the potential of PPG for pulse monitoring during CPR in a twelve pigs study. The PPG was extracted from the pigs′ nose simultaneously with arterial blood pressure signals, measured from the aortic arch, in order to validate the PPG results. The presence of spontaneous cardiac pulse was inferred based on PPG time traces and frequencies spectrograms. The results obtained, revealed that this approach could be promising to use for pulse monitoring during CPR. Nevertheless, the nose location (not representative of a good clinical practice) and the fact that it is an animal model, means that the results cannot be completely transposed for clinical cases. Another interesting approach is the one developed by Hubner et al. [50], it also uses PPG for pulse assessment, reinforcing its potential for CPR support.

Currently, the pulse monitoring techniques established in clinical practice include PPG, bioelectrical impedance, ultrasonography and sphygmomanometry, all having gaps in terms of cost, size, accuracy and ease of application [16]. Additionally, the exclusive use of the ECG for pulse monitoring is also very limited, once its detection does not guarantee that the ventricular ejection of blood is enough to irrigate al the essential organs, namely the brain [16], [48]. A small heart contraction is sufficient to generate an ECG signal. Therefore, with high sensitivity and portability, low-cost, the use of the ACC sensor is an interesting approach for pulse presence monitoring during CPR [10].

Muehlsteff et al. in [16], developed an algorithm for pulse presence tracking, involving 27 patients submitted to HUTT test. The algorithm was based on activity level of the ACC signal, calculated based on its variance, and on the beats that fed a selectable either Linear or Support Vector Machine classifier that identifies the pulse presence in each 10 second periods. Placing the ACC sensor at the carotid artery, it was observed that the ability of this sensor to reliably track the pulse in a conscious patient may be compromised, since it is very susceptible to motion artifacts. Nevertheless, for a patient at rest, without any movement, the pulse presence was accurately monitored. Since during CPR the person is unconscious, it is legitimate to assume that this approach might exhibit potential for pulse presence detection during resuscitation.

A more direct approach to CPR was the one developed in [10] by Dellimore et al. The algorithm was applied in a database collected from patients undergoing CPR. It classifies the signals based on its activity level, using the standard deviation, periodicity, and the prominence of the largest peak in a 3 seconds autocorrelation window. Despite the good performance achieved for activity level classification, the periodicity assessment accuracy was low. However, it demonstrated that the principle had potential for CPR application.

3.5. Conclusion

In this chapter was introduced the main approaches found in literature for continuous blood pressure assessment, syncope prediction and pulse assessment during cardiopulmonary resuscitation, as well as the shortcomings of those approaches. It aimed to clarify the challenges that this work faced and the gaps that it addresses using an accelerometer sensor as an interesting and promising modality for pulse assessment during CPR and syncope prediction.

Chapter 4

Artifact detection in Accelerometer Signals from the Carotid

4.1. Introduction

NMS patients suffer from hypotension and/or bradycardia, which result in cerebral hypo-perfusion and can finally lead to a sudden, transient loss of consciousness with spontaneous recovery [51]. As we have already mentioned, NMS is associated with a higher risk of falls, which is in particular a problem in the elderly. It compromises quality of life, is one of the root causes for injuries due to falls and therefore causes financial costs to the healthcare system [51]–[53]. Effective early warning systems for the management of high risk populations, which are able to predict an impending NMS event via the assessment of pulse strength and by monitoring trends in surrogate blood pressure parameters, is a highly relevant and interesting area for innovations.

Regarding the cardiopulmonary resuscitation, manual palpation is still the most basic approach to check for pulse presence in an unconscious patient. The procedure consists of placing a finger above an artery close to the skin surface such as the carotid, femoral or radial artery and to feel the pulsations. Palpation which is still the "golden reference" for pulse check has been shown to be error prone and often takes too long during cardiopulmonary resuscitation [12]–[15]. Therefore, palpation-based pulse checks by layman are not recommended anymore in emergency care guidelines. Due to this fact, there is a need for a sensing modality, which is 1) easy to apply in demanding stressful situations, 2) can objectify and preferably quantify pulse presence and 3) can be understood by consumers for acceptance.

Therefore, an interesting sensing modality for both problems mentioned is the accelerometer sensor, which has found widespread use in many consumer applications. Low cost, low power, small and inexpensive sensors with high sensitivity are available. They enable sophisticated signal processing techniques such as for noise and artifact reduction via signal fusion techniques [54], [55], for motion detection and classification

as required in many sports modalities (e.g., in swimming) [56], but also for vital sign and context measurements. An ACC sensor may provide a means of objectifying pulse palpation, which has been demonstrated in previous works on the basic feasibility of ACC-based pulse detection from signals acquired from the carotid artery [10], [16], [28], and also have potential for features extraction for syncope prediction.

Despite of the aforementioned, the ACC signal is prone to various sources of error (e.g., motion artifacts), which can complicate the extraction of reliable vital sign parameters and compromise the utility of the ACC in healthcare applications. Thereby, it is very important to detect those sections of the signal, which are contaminated by artifacts in order to remove these sections from further processing. In this chapter, the goal is to assess the ability of different simple features to capture these artifacts in ACC signals obtained at the carotid. It is introduced a systematic analysis of the detection performance based on low computational complexity features that can be easily integrated into embedded systems as required in portable Health applications as well as in resuscitation systems. A simple threshold-based classifier is proposed to detect artifacts in ACC signals collected from the carotid.

4.2. Methods

4.2.1. Experimental Protocol and Setup

To develop and test the methodology a data collection study was performed with 12 healthy volunteers. The protocol was designed to capture typical artifacts to be expected during daily life activities (e.g., head and neck movements, talking, swallowing, etc.), but also extreme situations such as jumping (simulation of rapid body movements). Specifically, the protocol consisted of five phases without any noise (two in the supine, two in the seated positions and one in the standing position), and five phases characterized by a specific movement such as: arm movements in the horizontal position, speech, rotation of the neck, swallowing and jumping. Each of these phases had a duration of 20 seconds and were separated from each other by a transition phase of 10 seconds.

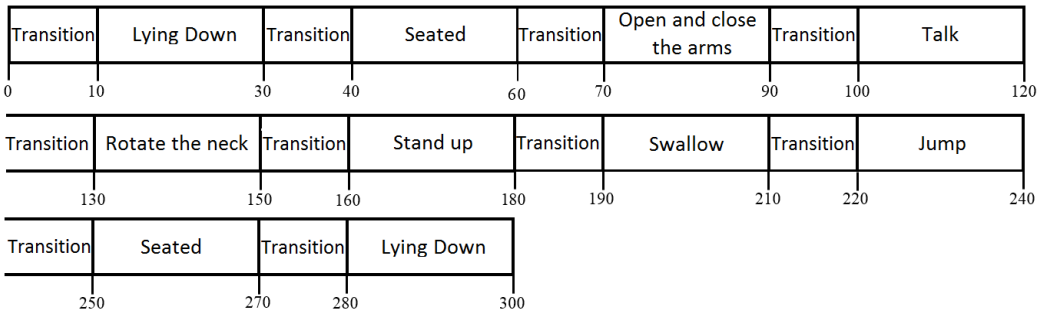

Figure 10 - Description of the data acquisition protocol activities/phases and respective duration (seconds).

The acquisition process for each subject had a total duration of 300 seconds (5 minutes) as illustrated in Figure 10. One example of a signal stream generated by this procedure is shown in Figure 11. The Data was recorded from twelve healthy volunteers that provided informed consent. The age of the participant group was 29±11 (mean ± SD) years (from 22 to 49 years) and body mass index (BMI) was 23.28±2.02 kg.m^{-2} (mean ± SD).

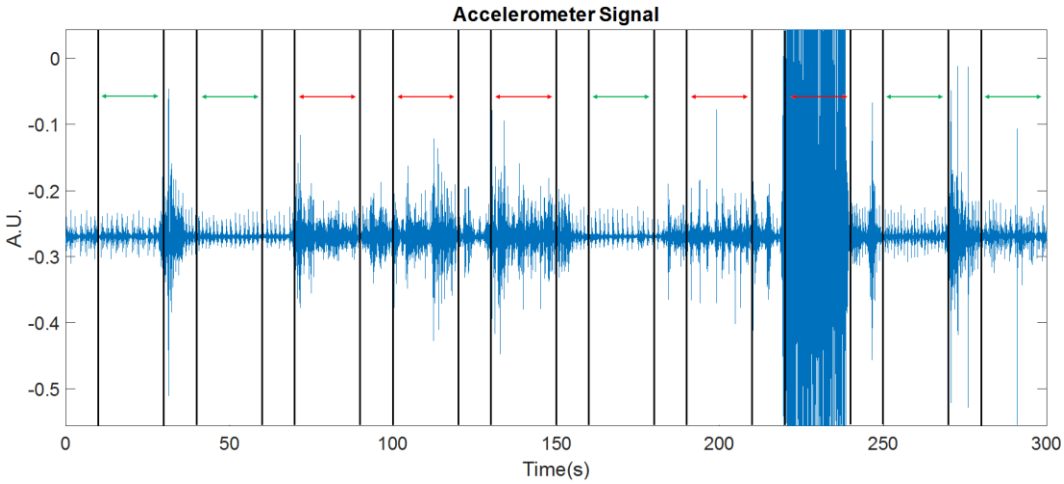

Figure 11 - Representation of a generated ACC signal (patient 12); segments signalized with the green arrows represent clean phases and segments signalized with the red arrows represent noisy phases.

The accelerometer signals were acquired from the carotid with a multi-parameter, battery operated device called "SENSATRON" [57]. The three-axis ACC signals were collected with a sampling frequency of 62.5 Hz. The absolute value of the acceleration vector (Abs. ACC) was also extracted using (8), where ACC_X, ACC_Y and ACC_Z represent each of the individual accelerometer axis and n represents the sample index.

$$Abs.ACC(n) = \sqrt{\left(ACC_X(n)\right)^2 + \left(ACC_Y(n)\right)^2 + \left(ACC_Z(n)\right)^2} \quad (8)$$

Simultaneously, an ECG was measured, sampled at 250 Hz. The location of the accelerometer and the "SENSATRON" layout can be observed in Figure 12.

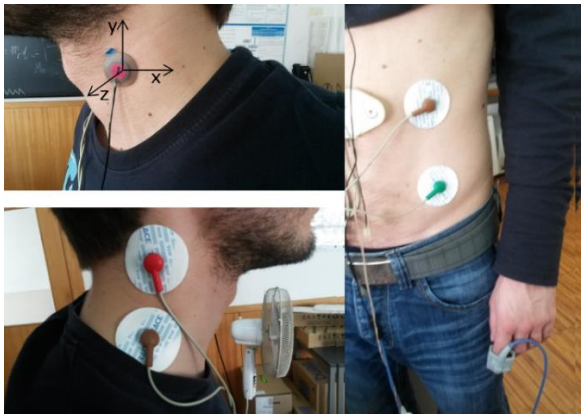

Figure 12 - Location of the accelerometer (top left). The ECG sensors of the "SENSATRON" (bottom left and right). More details about the system can be found in [57].

4.2.2. Implemented Algorithm for Signal Classification

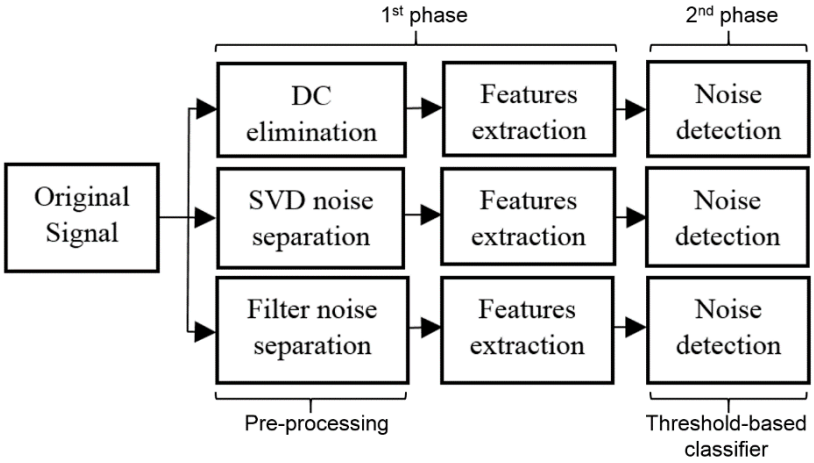

Figure 13 - Scheme of the different steps of the algorithm.

Figure 13 depicts the tested solutions for the artifacts detection in ACC signals. The classifier algorithm based on a classical training and testing approach was developed using six different features. The implemented processing stages comprise two distinct phases. In the first phase the extraction of the signal features was performed. In the second phase, a simple threshold-based classifier was applied, for which the optimal threshold was determined during a training phase based on a receiver operating characteristic (ROC) analysis. The performance of the classifier was evaluated using a test-data set. Furthermore, features relevance was assessed using a features selection score metric [43] in order to evaluate features providing complementary information to be integrated into a more robust multi-feature classifier.

1st Phase: in the first phase, each of the axis of the ACC signal was pre-processed for feature extraction using three different approaches depicted in Figure 13. It was filtered with three different high-pass filters. In the simplest pre-processing stage, a 5th order Butterworth high-pass filter with cut-off frequency of 0.5 Hz was applied in order to eliminate the DC component as well as frequencies related to respiratory cycle or vasomotion. In the others two pre-processing stages the rational was to isolate the noise content from the actual carotid pulse induced acceleration signal and to extract features from the former. Using the Singular Value Decomposition (SVD) approach, it was selected the less relevant portion of the signal defined by the data. Applying the high-pass filter with higher cut-off frequency it was selected the high-frequency noise component. This is based on the observation that movement artifacts tend to exhibit higher frequency components compared to the non-disturbed carotid signals, as it is clearly demonstrated in Figure 14.

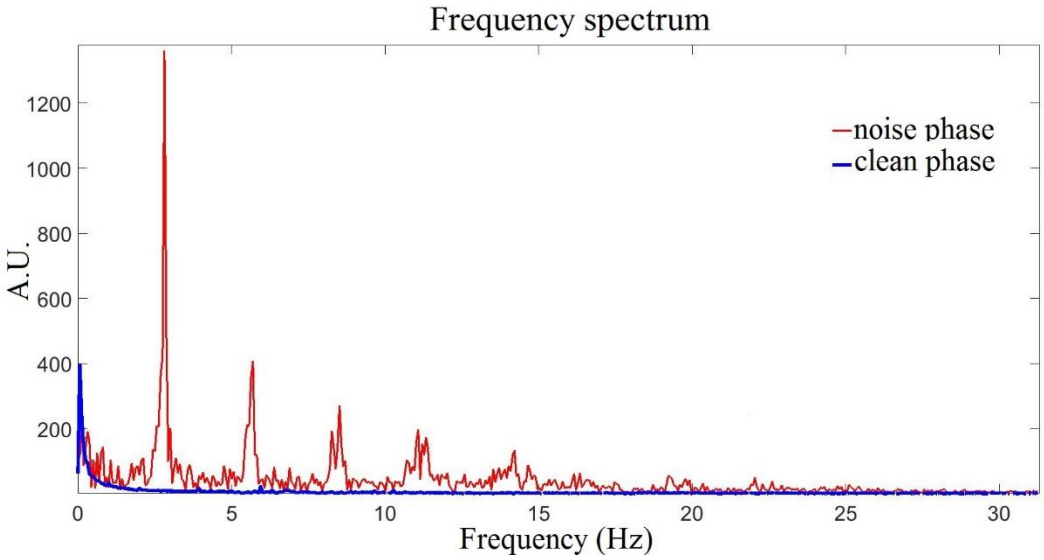

Figure 14 – Representation of the frequency spectrum of patient 8 in two different phase: noisy phase with the red label and a clean phase with the blue label.

In the filter-based noise separation approach, the cut-off frequencies were determined using a simulation modelling radius variation of the carotid artery given a typical blood pressure of SBP = 120 mmHg and DBP = 80mmHg [22]. The heart rates considered as input in the model were at rest, 80 bpm (average value of the heart rate at rest [58]), and during the resuscitation, 240 bpm [59]. The pulse pressure wave was simulated using the model reported in [28], partially explained in the previous chapter. Basic blocks of the simulation model are depicted in Figure 15. Using this approach, the actual cut-off frequencies were determined as 5.4 Hz and 16.0 Hz given that these frequencies

correspond to the expected accelerometer signal bandwidth at 80 bpm and 240 bpm, respectively.

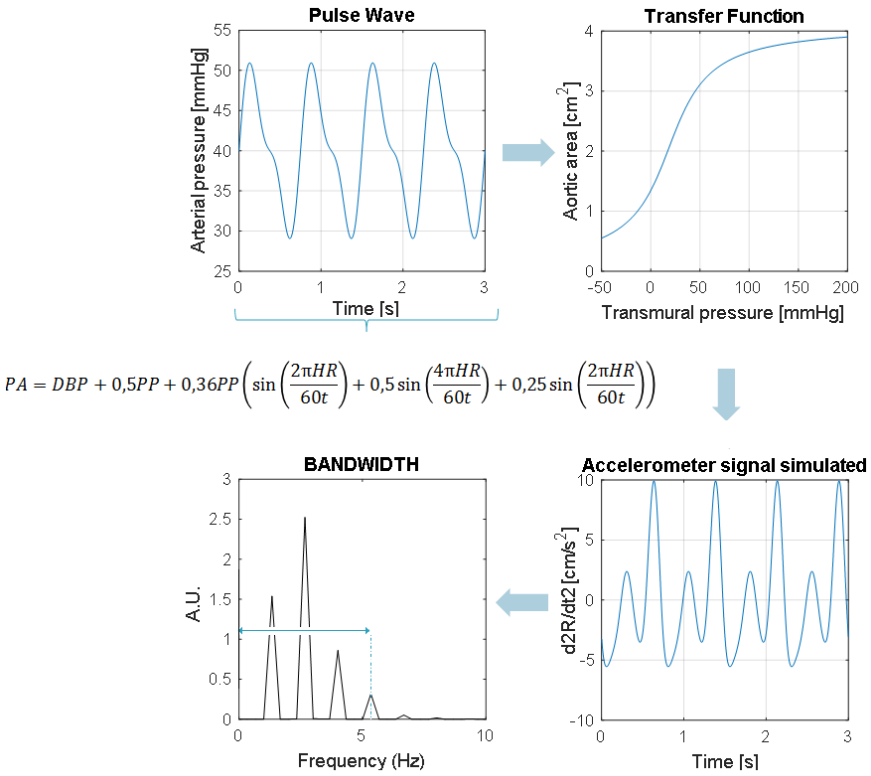

Figure 15 - Scheme of the simulation model for 80 bpm. PA-arterial pressure; DBP-diastolic blood pressure; PP-pulse pressure; HR-Hear rate; t-instant of the pulse.

In the second noise separation approach the SVD method is applied in order to identify signal components related to noise. Let $A \equiv (x_x, x_y, x_z) \in \mathbb{R}^{nx3}$ with n the number of samples, be the matrix formed by appending the three axis of the accelerometer signal, decomposed in three matrix, according to the following equation:

$$A = USV^T \tag{9}$$

where the columns of the matrix V and U consist of the right and left singular vectors, respectively, and the S is a $3x3$ diagonal matrix whose diagonal are the singular values of A [60]. Each singular vector represents one of the orthogonal vectors describing the space spanned by the signal. However, the relevance dimension to reconstruct or describe the signal is different. As Figure 16 illustrates, the first is significantly more relevant than the other two, representing during the entire extraction, the most part of the signal. The third one, is also less relevant than the second.

The relevance was calculated according to:

$$Relevance_i = \frac{SV_i}{\sum SV} \tag{10}$$

with SV_i representing the i^{th} singular value and $\sum SV$ the sum of the three singular values.

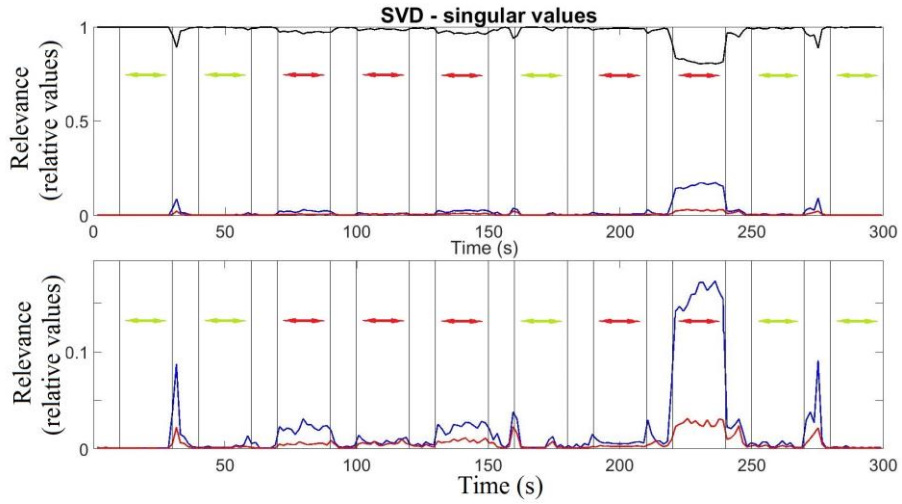

Figure 16 – Representation of patient 8 singular values relevance during the extraction period. The first one with the black label, the second with the blue label and the third with the red label. Upper graphic: representation of the three singular values; Bottom graphic: representation of the second and third singular values. The green and red arrows represent the phases with/without noise, respectively.

Therefore, assuming that the noise represents an uninteresting part of the signal, to isolate it, the two major singular values were zeroed and the matrix A recalculated according to formula (9).

In a next step, from these pre-processed signals the 6 different features (Energy Mean - EM, Energy Variance - EV, Shannon Energy - SHE, Third and Fourth Statistical Moments to assess peakness and skewness of the signal distribution – SM3; SM4, and Teager Energy - TE), were extracted as defined in the following equations:

$$EM = \frac{1}{N_s}\sum x(n)^2 \tag{11}$$

$$EV = \frac{1}{N_s}\sum \left(x(n)^2 - E_\mu(n)\right)^2 \tag{12}$$

$$SHE = \sum [x(n)^2 log(x(n)^2)] \tag{13}$$

$$Statistical\ Moment = \sum \frac{x(n)^t}{N_s} \tag{14}$$

$$TE = \frac{1}{N_s}\sum (x(n)^2 - x(n-1)x(n+1)\ ) \tag{15}$$

where x represents the signal, n represents the sample index, t represents the order of the moment (3rd or 4th) and N_s the number of samples on the moving window. These features were calculated using a 1.5 seconds centered moving window with 99% of overlapping. All the features were normalized, by the mean of the signal amplitude acquired during the first lying down phase of the protocol.

2nd Phase: in this phase, the threshold-based classifier was tuned using a training dataset to estimate the optimal threshold using a ROC-approach. Performance was evaluated using an independent test dataset. The signals collected from the volunteers were randomly divided into these two groups to form the aforementioned datasets, i.e., the training dataset was defined using the data collected from two thirds of the available individuals (8 subjects randomly selected), whereas the test dataset was constituted by the signals collected from the remaining individuals (4 subjects).

As was already mentioned, a ROC-based approach was applied using the training dataset in order to obtain the optimal threshold for each feature, i.e., the selected threshold value is the one that optimizes the tradeoff between sensitivity and specificity (see Figure 17). It should be noted that, in order to avoid influence of uncertainty during the prolonged transitions between adjacent phases in the protocol (e.g. due to slow reaction of the subject), the first and last 2 seconds of each phase have not been considered for classification performance assessment. Another important point to mention is that the ground truth of the signals was defined by manual classification according to the different phases of the protocol. This could affect the performance of the classifier.

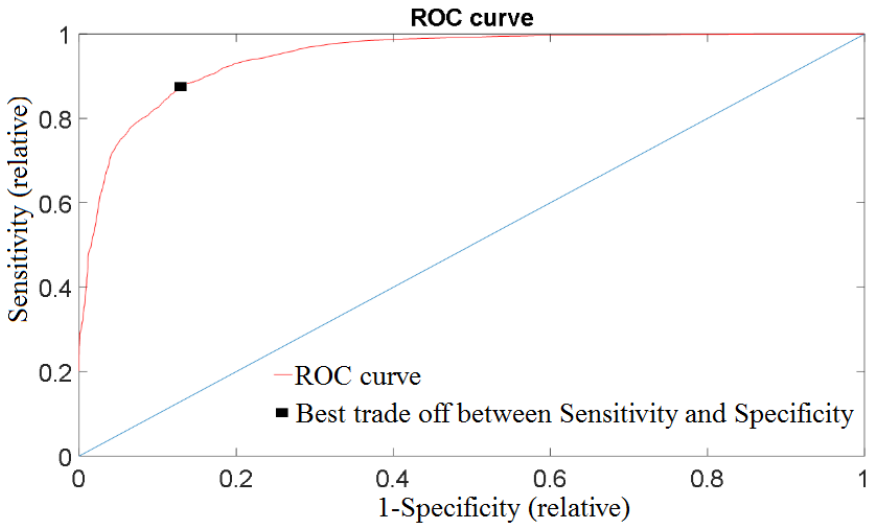

Figure 17 - Example of a ROC curve and the point associated to the best balance between Sensitivity and Specificity.

Finally, there was the ranking of the most convenient features for the classifier, based on FSS-score, that combines their relevance, by the area under the ROC curve (AUC), and redundancy, assessed by Spearman's rank correlation coefficient (RCC) [43]. This allows to know which feature is more adequate to define a classifier, and also which features provide complementary information. Thus, the most suitable features for a multi-feature classifier can be selected based on this ranking. It was calculated according to following formula:

$$FSS_i = AUC(F_i) - \frac{\left|\sum_{F_j \epsilon S} RCC(F_i, F_j)\right|}{|S|} \tag{16}$$

with *AUC(Fi)* representing the AUC obtained by the i^{th} feature, *RCC* (FT_i, FT_j) the Spearman's RCC between the i^{th} and j^{th} feature, *S* representing the subset of selected features at each iteration and |*S* | its cardinality [14].

4.3. Results and Discussion

4.3.1. Implemented Algorithm for Signal Classification

Table I shows the best performance results to discriminate noise/no noise achieved using each of the individual accelerometer axis (ACC_X, ACC_Y and ACC_Z), the Abs. ACC and the classification approach outlined in the previous section.

Table I - The best performance for the three different axis and the absolute value of acceleration.

AXIS	ACC_X	ACC_Y	ACC_Z	ABS. ACC
SEN (%)	82.1	76.2	91.1	88.7
SPE (%)	93.5	94.3	91.3	92.2

According to Table I, the component that provides the best performance for the classifier was the component on the direction z (perpendicular to the skin- see Figure 12). Looking into the performance of each patient of the test group, according to Table II, the most consistent and constant axis was ACC_Z, always with values of SEN and SPE above 80%. Even in the case of patient 2, the ACC_X, ACC_Y and Abs. ACC had values of sensitivity of 43.5%, 47.3% and 68.3% respectively, whereas the ACC_Z achieved 87.4% making this axis more reliable for noise discrimination according to the algorithm applied.

Table II –Algorithm performance for each patient of the test group.

	PATIENT 2				PATIENT 6			
	ACC_X	ACC_Y	ACC_Z	Abs. ACC	ACC_X	ACC_Y	ACC_Z	Abs. ACC
SEN (%)	43.5	47.3	87.4	68.3	98.0	90.7	96.5	98.8
SPE (%)	97.6	98.2	96.7	97.5	88.2	90.6	87.5	87.3
	PATIENT 7				**PATIENT 12**			
	ACC_X	ACC_Y	ACC_Z	Abs. ACC	ACC_X	ACC_Y	ACC_Z	Abs. ACC
SEN (%)	98.4	90.0	100	99.8	88.4	86.8	80.4	88.1
SPE (%)	91.5	93.0	83.8	87.1.	96.4	95.2	97.3	96.6

In the following, taking into account the performance of each axis and the abs. ACC, only the results related to the z axis ACC and the absolute ACC value will be presented and discussed. In Figure 18, it is notorious the difference of energy between the various phases of the signal, where the contaminated segments exhibit much higher energy than the clean segments. As can be observed, interferences on the ACC signal are reflected as an increase of the signal energy. Specially, during the jumping phase, between the second 220 and the second 240, where the movements are much more aggressive than in any other phase, the energy reaches considerably higher values.

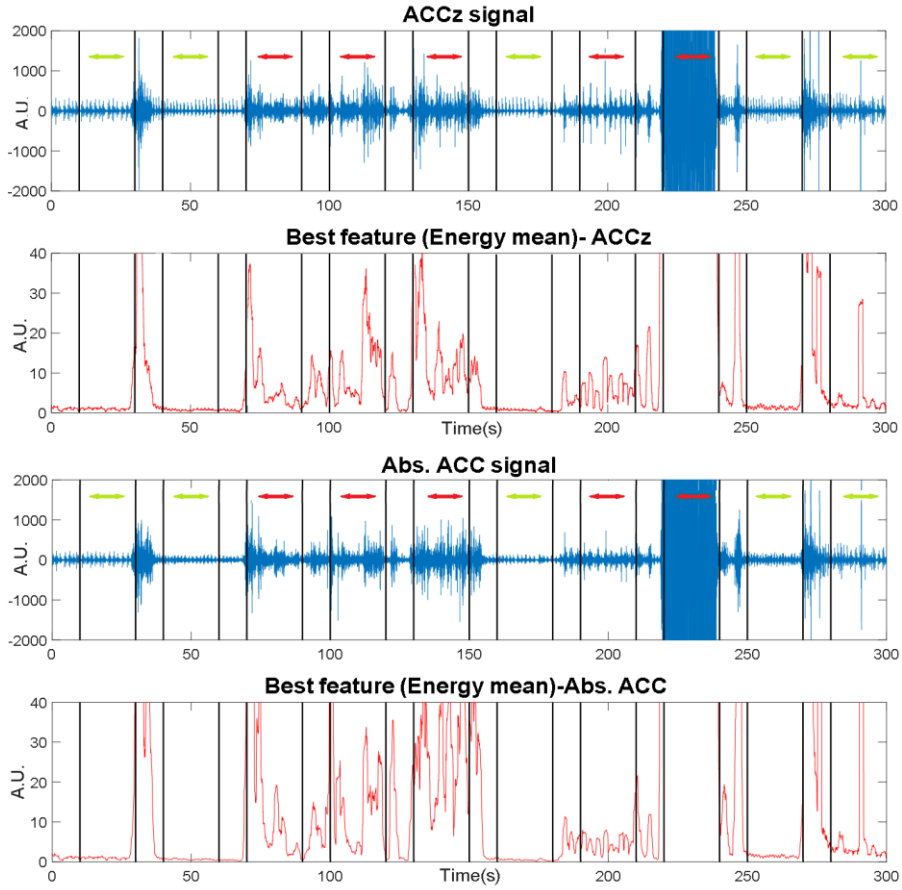

Figure 18 - Representation of Abs. ACC and ACC_Z signals, and respective energy for patient 12. The green and red arrows represent the phases with/without noise, respectively.

Table III, summarizes the classification results in the test dataset achieved using the aforementioned noise detection approach for the various pre-processing configurations and derived features. Very similar results for the best feature were obtained using the z-axis, with SEN=91.1% and SPE=91.3%, and using the absolute value of ACC signal, with SEN=88.7% and SPE=92.2%.

Table III - Classifier performance for all features, for the dimension z selected and for the absolute value of the acceleration.

PRE-PROCESSING TYPE\ FEATURE			**EM**		**EV**		**SM3**		**SM4**		**SHE**		**TE**	
			SEN (%)	**SPE (%)**	**SEN (%)**	**SPE (%)**	**SEN (%)**	**SPE (%)**	**SEN (%)**	**SPE (%)**	**SEN (%)**	**SPE (%)**	**SEN (%)**	**SPE (%)**
DC-FILTER		**ACC z**	80.2	92.0	74.6	89.7	70.6	90.1	72.3	91.1	75.1	89.5	83.6	93.3
		Abs. ACC	88.2	91.0	73.2	92.5	82.5	91.0	71.8	94.0	71.5	94.0	81.9	94.0
SVD		**ACC z**	62.3	95.6	62.7	93.9	63.6	91.7	62.9	94.1	61.9	94.1	58.9	94.4
		Abs. ACC	81.0	90.4	59.9	93.2	67.6	91.2	60.8	92.0	60.3	93.1	69.7	93.4
NOISE-FILTER	**fc=5.4 Hz**	**ACC z**	**91.1**	**91.3**	73.7	91.9	74.8	86.5	78.1	91.6	77.5	91.6	88.8	91.5
		Abs. ACC	**88.7**	**92.2**	75.9	91.9	83.8	92.0	78.8	92.2	78.1	92.3	85.2	92.4
	fc=16 Hz	**ACC z**	74.5	89.1	70.1	87.6	71.1	74.7	72.4	86.8	74.0	84.9	74.5	88.9
		Abs. ACC	74.6	93.4	70.5	89.0	72.4	92.6	73.3	89.9	73.3	89.6	74.5	91.5

Despite the relatively similar performance, as can be observed in Figure 6 (Chapter 2), in fact the carotid artery in its extension, is almost entirely parallel to the necks surface, which suggests that movements of dilation and constriction by the artery are more pronounced in the direction perpendicular to the skin of the neck. Considering that the signals induced by these movements are those of interest to be detected by the accelerometer, the optimal direction to the extraction in order to have a better signal morphology with higher quality, is the direction of the axis z. Therefore, in order to avoid the influence of other axis contaminations, all the further considerations are about the ACC_Z.

As Table III depicts, for most of the features, the pre-processing that led to the best results were the one derived with a high-pass filter (fc=5.4 Hz), with significant differences of the performance between the two cut-off frequencies used. These discrepancies might be caused by the fact that acquired data were from healthy people only doing regular and low-intensity exercises, therefore, the heart rate was usually below

80 bpm. Although the difference between these two cut-off frequencies the energy mean feature tends to provide stable results for a significant range of cut-off frequencies, with sensitivity and specificity values above 85 % until frequencies around 10.5 Hz, as it is illustrated in Figure 19.

A similar observation was found for TE. This feature exhibits good performance even when no noise filtering was applied, maybe due to the fact, that this feature is sensitive to both intensity and frequency of the signal, while all the others are more sensitive to the intensity.

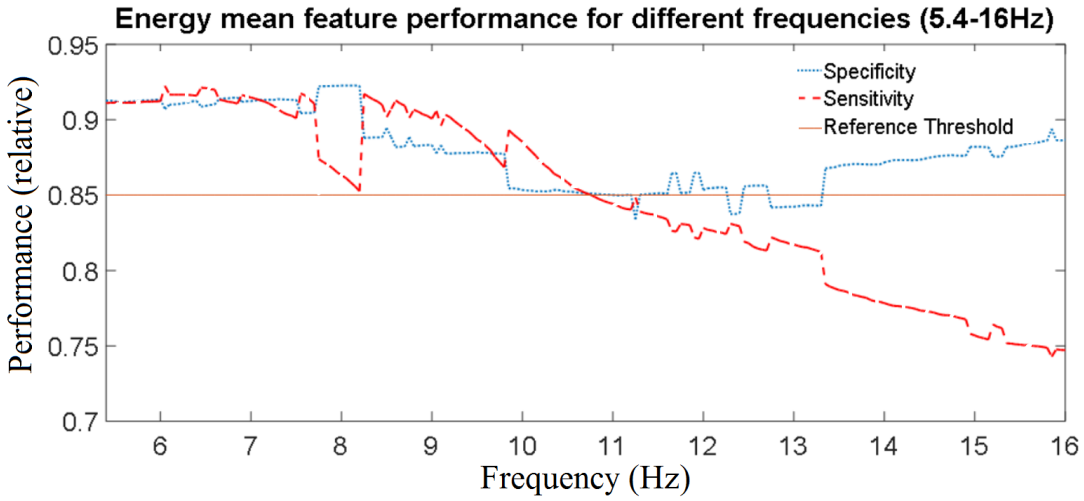

Figure 19 - Performance of Energy mean feature for different frequencies from 5.4 Hz to 16 Hz.

In Table IV it is assessed the level of feature relevance using the FSS-score approach for the selected components. Although the TE exhibits a similar AUC value compared to the EM, it is ranked in a lower position compared to the SM3, due to its higher correlation with respect to the EM. Furthermore, only the EM and the SM3 feature exhibit a FSS-score higher than 50%. This suggests that the remaining assessed features do not contribute with relevant added information to describe the problem's domain. Therefore, they might be irrelevant if a more complex multi-feature classifier is to be designed for artifact detection in ACC signals measured at the carotid.

Table IV - Feature selection rank, of the axis z, according to the FSS-score.

FEATURE	SCORE (%)	AUC
ENERGY MEAN	94.78	94.78
3º STATISTICAL MOMENT	75.16	81.83
TEAGER ENERGY	40.77	94.11
4ºSTATISTICAL MOMENT	18.42	86.44
ENERGY VARIANCE	10.17	85.71
SHANNON ENERGY	-0.0227	78.4

4.4. Conclusion and Future Work

In this chapter it was investigated the application of low computational complexity features in the detection of movement artifact in accelerometer signals acquired from the carotid. Using a dataset collected from healthy subjects, it is shown that very promising results can be achieved with a simple feature as the first statistical moment of the signal energy, with sensitivity and specificity above 90%. However, it would be interesting to develop a more robust multi-feature classifier with the first and the third statistical moments, once they seemed to have a good complementarity.

The axis that has revealed the best performance was the axis z, being this the most consistent, reliable and stable, however a similar performance was achieved with the absolute values of the ACC signal.

Despite the similar performance, the signal of interest to extract is the movement of dilation and constriction by the carotid artery. Once these movements are more pronounced in the direction perpendicular to the skin of the neck, this direction is the optimal one to extract the signal with a better morphology and higher quality, which corresponds to the direction of axis z. Therefore, axis z seems to be the most propitious axis to use, although, the absolute value of the ACC signal also is an interesting alternative.

The limitations imposed by the reduced database available in this work do not allow to draw definitive conclusions or to perform any kind of generalization. In this way, the conditions imposed, namely the noise threshold used might have to be recalculated after a change of the database. In spite of this, the methodology developed and tested, revealed optimistic results. Consequently, the next step would be to apply it in a more extensive dataset collected using the target population of the intended core applications. Other directions for future work comprise (i) the assessment of the ACC signal quality in terms of diagnostic value during artifact contamination and (ii) to explore disturbance of the quasi-periodic nature of pressure pulses in order to detect artifacts.

Chapter 5

Robust Carotid Pulse Detection Using Accelerometry and Electrocardiography and Pulse Arrival Time Extraction

5.1. Introduction

This chapter builds on top of the developments introduced in the previous chapter by exploring the properties of the ACC sensors in order to move a step further to the resolution of the problems that CPR process and syncope prediction face.

Due to the high costs in healthcare related to syncope, especially those caused by falls in the older population, and due to the impact it has on the quality of life of the population, an effective early warning system able to predict impending NMS event via the assessment of surrogate blood pressure parameters, is a highly relevant and interesting area for innovations.

Regarding CPR, its efficiency and velocity are a crucial factor for the sequelea that may arise from a cardiac arrest or between life and death [9]. Hence, any phase of the resuscitation process must be optimized so the damages can be the least possible. Taking into consideration that, the method for pulse detection during CPR is unreliable and error prone, an automatically and reliable pulse presence detection mechanism is highly appropriated and needed [10], [16].

Therefore, knowing the potential of ACC sensors in both areas and taking into consideration the susceptibility of ACC signals for noise contamination, a noise classifier algorithm was developed in the previous chapter. After this, the next step should be the elaboration of an algorithm for pulse presence identification and subsequently BP surrogate features extraction for syncope prediction. Taking into account the

contaminated samples, the segments with pulse presence are detected, from which, the BP surrogate features are inferred. In this way, the aim of this study was to perform a first initial investigation of a signal fusion concept between ECG and ACC signals inspired by calculating a cross-correlation feature for discrimination of pulse presence/absence as described in [61] and to extract and infer PAT as a Blood Pressure surrogate feature using the ACC signal.

5.2. Methods

5.2.1. Experimental Protocol and Setup

As in chapter 4, the data collection study was performed using the investigational device "SENSATRON" from Philips [16]. This bio-signal acquisition platform enables the synchronous measurement of ECG signals and multiple three-axis ACC signals. In this experiments, one of the ACC sensors has been positioned on the carotid (see Figure 12 - Chapter 4). The three-axis ACC signals were sampled at 125 Hz, and the ECG signal at 250 Hz. Since the main interest is in the artery dilation signal, this analysis was focused just in the signal from ACC z-axis, as it is explained in Chapter 4.

The analysis is based on a subset of data gathered during HUTT test involving 27 patients with an unexplained history of syncope [16]. Data of 8 patients, 5 male and 3 female, with an average age of (56 ± 23) years and a BMI of (26.5 ± 5.6) kg.m-2 were used in this work. These patients had different cardio-vascular conditions such as arrhythmias or structural heart diseases.

Since HUTT test data typically does not include well-defined phases without pulse information, in order to have a ground truth of segments with/without pulse presence for the development of the pulse presence classifier, it was induced in the database segments of ACC signals without pulse information obtained during lab tests. This data set was collected using the ACC sensor of the "SENSATRON" device by (i) attaching the sensor on the back of a hand to simulate the absence or a low power pulse signal, and (ii) placing the ACC sensor on a table (sensor is not attached at all). These segments representing "Pulse absence" were placed randomly in the HUTT test dataset. Each "Pulse absent" phase has a duration of 5 minutes, in which any external disturbance was avoided. One signal stream generated by this procedure is shown in Figure 20. It is

important to notice that, this replacement of ACC signal segments was used just for the pulse presence classifier development. For the PAT extraction, the ACC was used without any kind of induced segments.

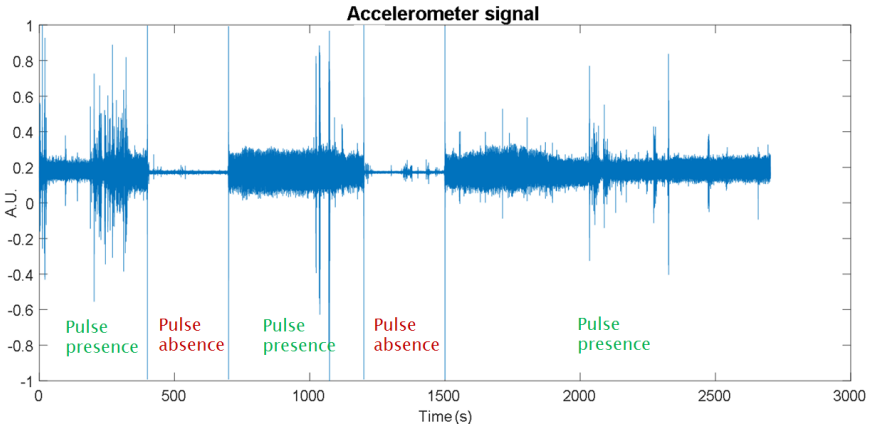

Figure 20 - Representation of a generated ACC signal (patient 1); segments between the blue vertical lines represent phases with (green label) or without (red label) pulse.

Not all available data for this study exhibited adequate characteristics for processing. It is observed that patient 2 experienced severe atrial fibrillation during the HUTT test collection procedure, resulting in ACC signals of low signal-to-noise (SNR). The ECG of patient 5 was considerably contaminated with power line noise and patient 8 contained Premature Ventricular Contractions (PVCs), reflecting on an ECG and ACC signals considerably affected, as shown in Figure 21. In the case of patient 7, the ACC signal is also considerably contaminated. In certain segments the pulse can be easily identified, but the morphology of the pulse had suffered significant interference, as occurs with patient 6, which may affect the cross-correlation (see Figure 22). These issues might compromise the performance of the algorithm, although illustrate the broad range of situations that the method will face and should be able to handle in a real-life application.

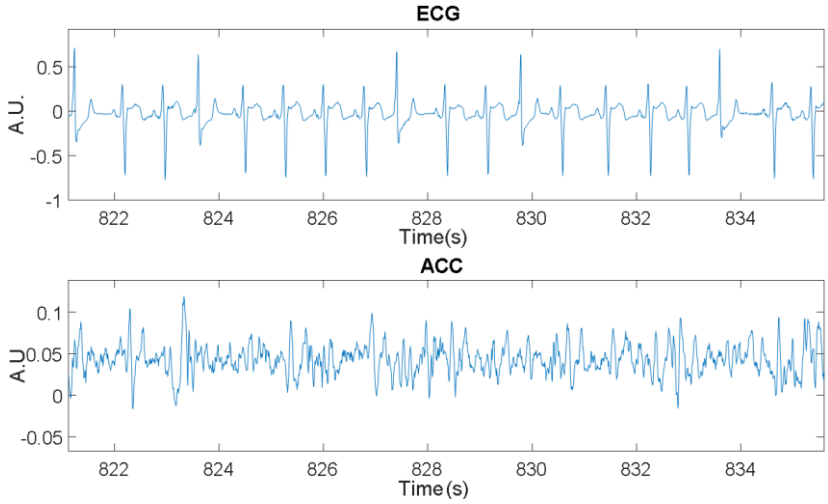

Figure 21 - Premature Ventricular Contractions in Patient 8.

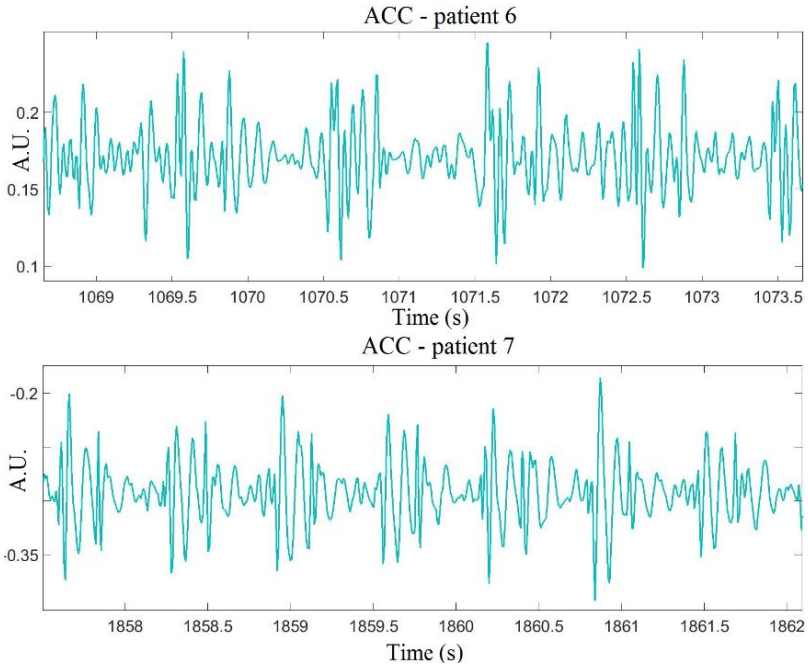

Figure 22 – Representation of the ACC signals of patient 6 (top) and patient 7 (bottom).

Regarding the patients 1, 3 and 4, the signals had revealed a good quality signal with good morphology and high SNR.

5.2.2. Implemented Algorithm for Pulse Presence Classification

The proposed method for pulse detection is depicted in Figure 23. The main idea of the algorithm was to explore a signal fusion concept of the ACC and ECG signals in order to infer pulse presence during the ACC signals. The first stage of the algorithm identified noise due to body movement, speech and head movement using the method as reported in Chapter 4. This noise detection method was tuned for the presence of high-frequency or high intensity interferences in the carotid ACC signal. In the second processing stage a correlation feature from pre-processed ECG and ACC signals was derived from sliding windows [61]. Finally, in phase three, a simple threshold-based classifier was applied to detect pulses. The optimal threshold was identified using an ROC approach on the training data.

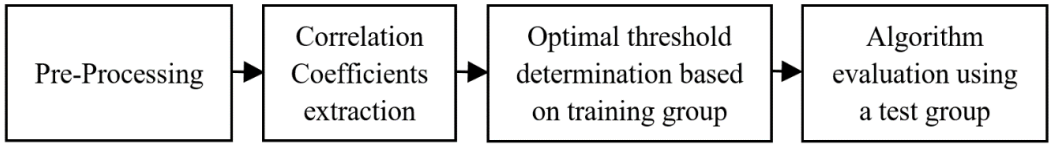

Figure 23 - Main stages of the proposed algorithm.

These phases are described in detail below:

1st Stage: This stage prepares the ECG and ACC signals for the correlation assessment. For this purpose, the ECG signal was resampled at 125 Hz to have the same sampling frequency as the ACC signal. Subsequently a 5th order Butterworth high-pass filter with a cut-off frequency of 0.5 Hz was applied in order to eliminate baseline noise. In a next step, two parallel procedures were implemented for the ACC signal: (i) the signal was high-pass filtered (details below) and (ii) the noise in the ACC signals was detected per sample and annotated in order to avoid further processing (see Figure 24). The percentage of signal contamination for each patient was calculated according to (17).

$$Contamination\ (\%) = \frac{|total\ number\ od\ contaminated\ samples|}{total\ number\ of\ samples} \times 100 \quad (17)$$

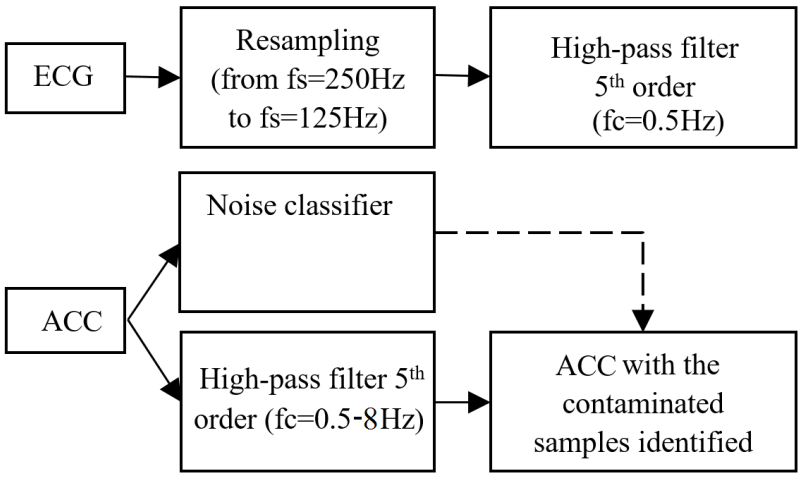

Figure 24 - Scheme of the different pre-processing steps, with fs representing the sampling frequency and fc the cut-off frequency.

The ACC signal was high-pass filtered using a 5th order Butterworth filter with a cut-off frequency higher than 0.5 Hz to eliminate the DC component as well as any type of low-frequency contamination such as respiratory movements and vasomotion. Furthermore, an increase in the cut-off frequency highlighted the main peaks in the ACC signal, which were due to the carotid pulse and, therefore, improved the correlation with the ECG signal. As Figure 25 illustrates, applying a cut-off frequency of 5 Hz, contrasting to fc=0.5 Hz, the signal loses its low-frequency oscillations, presenting a morphology more similar to the ECG, which optimizes the cross-correlation and allows that more accurate results can be achieved. After this phase, the noise-contaminated sections of the ACC signal were identified, having little or no influence, for further processing.

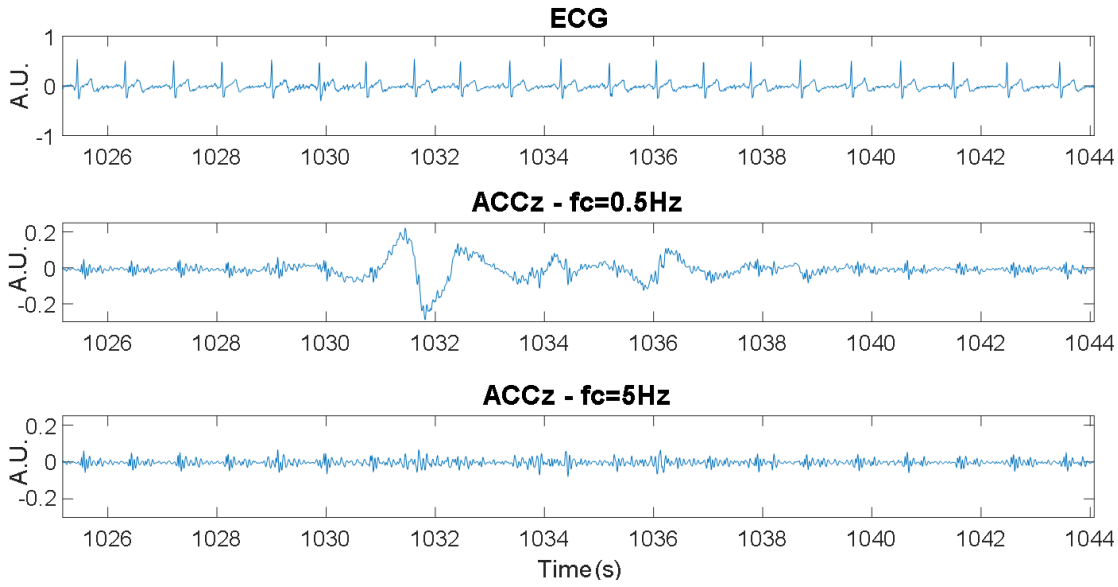

Figure 25 - ACC signal of patient 6 after a high-pass filter has been applied. Upper diagram: ECG; middle diagram: ACC submitted to a high-pass filter with a cut-off frequency of 0.5 Hz; lower diagram: ACC submitted to a high-pass filter with a cut-off frequency 5 Hz.

2nd Stage: In this stage, the correlation between the ACC and ECG was determined using a sliding window of width equal to 3 seconds and with 75% of overlap. From each window, the absolute maximum of the normalized correlation coefficients was extracted for further assessment of pulse presence (see Figure 26).

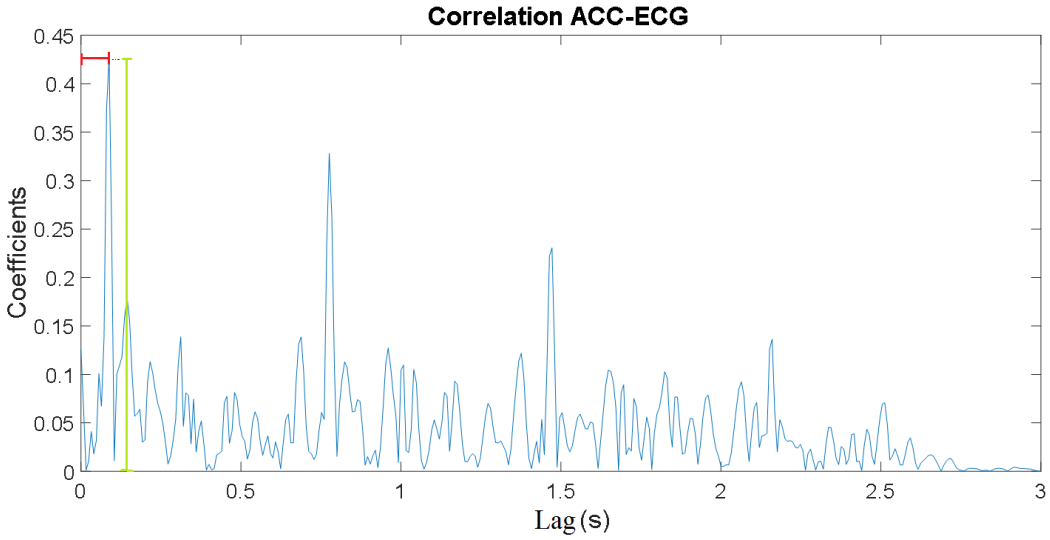

Figure 26 - Example of the cross-correlation coefficients for a 3 seconds window. The green mark represents the coefficient used for pulse classification and the red mark the lag considered as PAT.

In order to reduce noise interference, cross-correlation was only assessed if the percentage of contaminated samples in the analyzed window was below a pre-defined threshold L. After a careful and detailed analysis, it was observed that changes on the percentage L of contamination had only minor influence on the performance of the

algorithm and it was fixed to 20%, as it is observed in Table V. To minimize loss of samples, contiguous contaminated sections with less or equal to 10 samples were reconstructed using linear interpolation. For contiguous sections of contaminated ACC signals greater than 10 samples, the affected samples and their ECG counterparts were removed from further processing. For a better understanding, the process of how to deal with the noise during the cross-correlation features extraction is depicted in Figure 27. Figure 28 represents the correlation coefficients for two patients using the pre-processing steps discussed before.

Table V – Performance according to the change of contamination tolerated L, for a cut-off frequency of the ACC filter of 5 Hz.

***L* (%)**	**0**	**0.5**	**1**	**5**	**10**	**15**	**20**
SEN (%)	96.6	96.6	96.6	96.6	96.7	96.6	96.6
SPE (%)	94.9	94.9	94.9	94.9	94.9	94.9	94.9

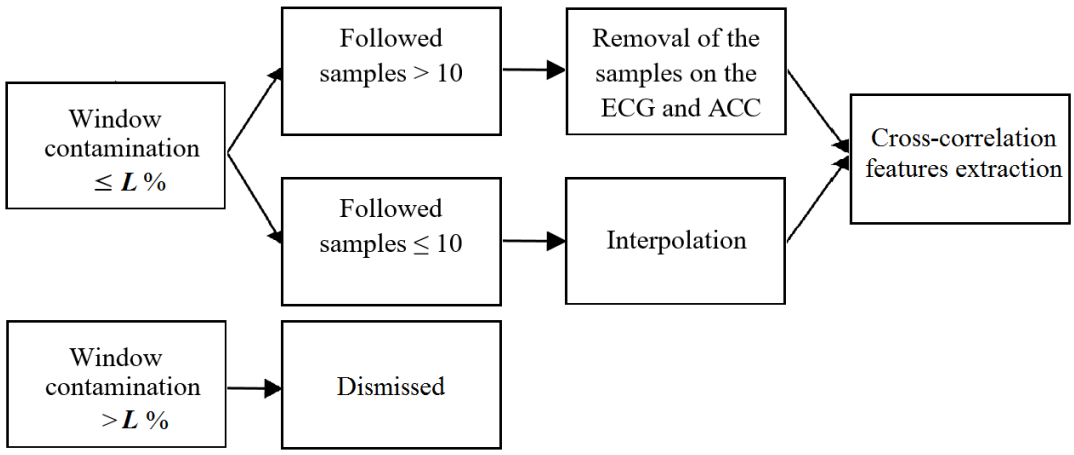

Figure 27 – Process for noise treatment during the cross-correlation features extraction

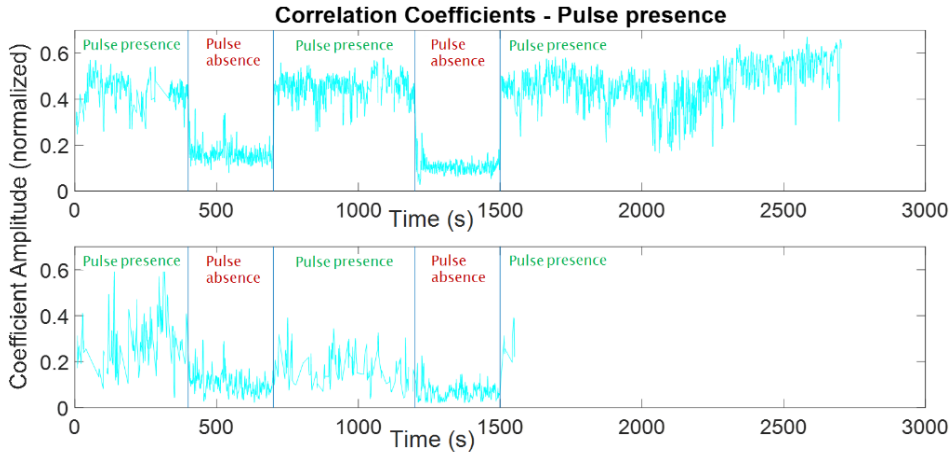

Figure 28 - Correlation coefficients extracted from the entire signal for two patients. Segments between the blue vertical lines represent the inserted "pulse absence" segments (Patient 1 - upper panel; Patient 5 - bottom panel; fc=5Hz; L=20%).

3rd Stage: In this stage, using an ROC-based approach, the optimal threshold was determined for a training dataset, i.e., the threshold that optimized the trade-off between sensitivity and specificity (see Figure 17 - Chapter 4), and then evaluated using an independent test dataset. The training and the test dataset were defined randomly at the patient level, i.e., two thirds of the patients in the database (5 subjects) were selected as part of the training group, and the remaining 3 patients formed the test group. The ground truth of these signals was defined by manual annotation.

To assess the optimal cut-off frequency for the high-pass filter applied to the ACC signal, the mentioned 3 phase's procedure, was applied for a range of frequencies between 0.5 Hz and 8 Hz. The upper limit of the interval was defined when an increase in the cut-off frequency was clearly reflected in a noticeable decrease of the algorithm's performance. For each frequency, the performance associated to the optimal threshold was annotated and posteriorly, comparing all the performances and using an ROC analysis, the optimal cut-off frequency was selected.

5.2.3. Implemented Algorithm for Pulse Arrival Time extraction

After the method introduced in the previous section has been applied, the optimal cut-off frequency for the ACC filtration and the optimal threshold for pulse classification were extracted, allowing the selection of the reliable signal segments for PAT inference, exploring the signal fusion concept of the ACC and ECG signals. Therefore, with 3 phases (see Figure 29), the present method also explores the ECG and ACC fusion to extract PAT and subsequently assess the relevance of this feature in a possible correlation with Systolic Blood Pressure. In the first phase, both ECG and ACC signals were high-pass filtered and the contaminated samples in the ACC signals identified. In the second phase, the correlation features from the pre-processed ECG and ACC signals were extracted, using sliding windows. In the last phase, the PAT extracted was filtered and then normalized for a subsequently correlation with SBP.

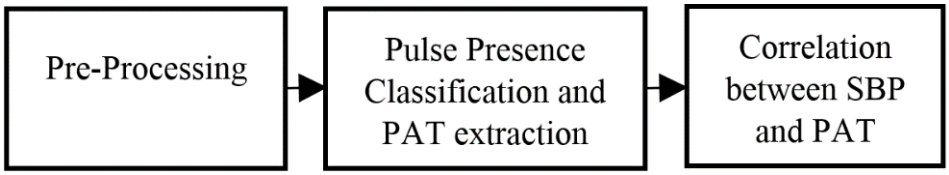

Figure 29 – Main stages of the presented method.

These phases are described in detail below:

1st Stage: in this phase, the signal was processed in an analogous way to the first phase of the previous method. The ECG was resampled at 125 Hz and high-pass filtrated with a cut-off frequency of 0.5 Hz, using a 5th order Butterworth filter. The ACC was also high-pass filtrated with the same type of filter, but the cut-off frequency used was the optimal one determined on the previous method. Afterwards, the contaminated samples were also identified.

2nd Stage: in this phase, the correlation between the ACC and the ECG was performed using a window of 3 seconds and 75% of overlap, as explained in the 2nd stage of the previous method. From each window, the absolute maximum of the normalized correlation coefficients was extracted, as was the associated lag (see Figure 26). If the coefficient value was greater than the optimal threshold, determined in the previous method, then the PAT (corresponds to the lag) was accounted for, otherwise it was neglected. In order to avoid causality problems, it was defined that the extracted PAT corresponds to the final instant of the correlation window considered (this might induce a delay to the signal). At this stage, the signal processing procedures with respect to noise were also the same as in stage 2 of the above method, i.e., the cross-correlation was only assessed if the ratio of contaminated samples was below 20 % of the window considered. Additionally, in order to minimize the loss of samples, for contiguous sections of contaminated ACC signal lower or equal to 10 samples, those samples were reconstructed using linear interpolation, for contiguous sections greater than 10 contaminated samples those samples were removed from further processing (see Figure 27).

3rd Stage: in this phase, after a complete extraction of the PAT, a 5th order Butterworth high-pass filter with a cut-off frequency of 0.005 Hz was applied, in order to smooth the signal, removing possible outliers. The value for the cut-off frequency was determined empirically based on which frequency better smooths and suits the signal (see Figure 30). Subsequently, it was normalized by the mean of the PAT value, during 1 minute of the first standing position (PATref). Then, after the identification of the syncope

event, given as the minimum SBP peak, the correlation between PAT and SBP was performed. For this, the region of analysis considered was from 3 minutes before the SBP minimum peak and the minimum peak.

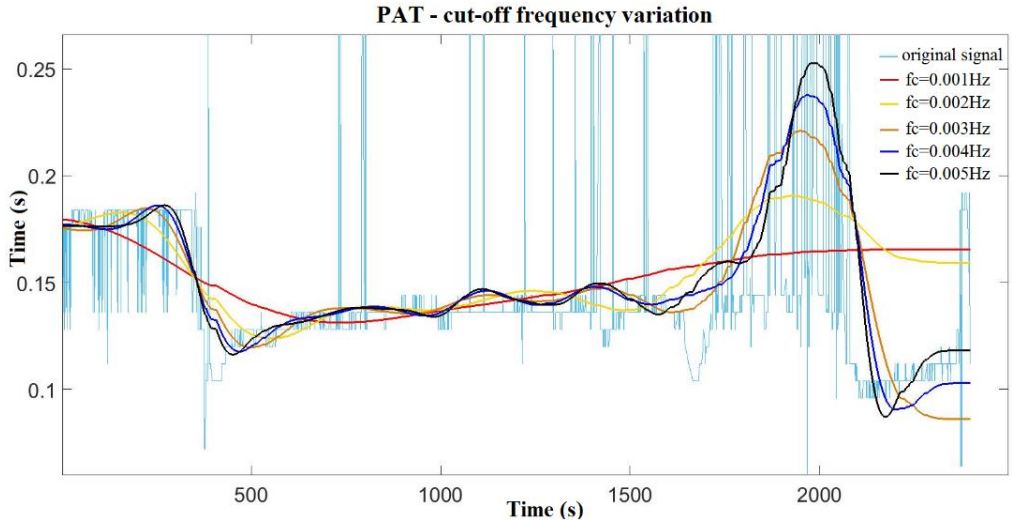

Figure 30 – Representation of the influence of the cut-off frequency in PAT values extracted.

In addition, 6 different reference values of PAT were analyzed since the moment that SBP began to decrease, until the SBP minimum peak (see Figure 31), in order to assess the changes in PAT values according to the SBP evolution. The reference values correspond to 0%, 5%, 20%, 50%, 80% and 100% ($PAT_{0\%}$, $PAT_{5\%}$, $PAT_{20\%}$, $PAT_{50\%}$, $PAT_{80\%}$ and $PAT_{100\%}$, respectively) of the time between those two events [1].

It is important to note that both the onset of the SBP decrease and the timing of syncope have been manually annotated, which may induce some error.

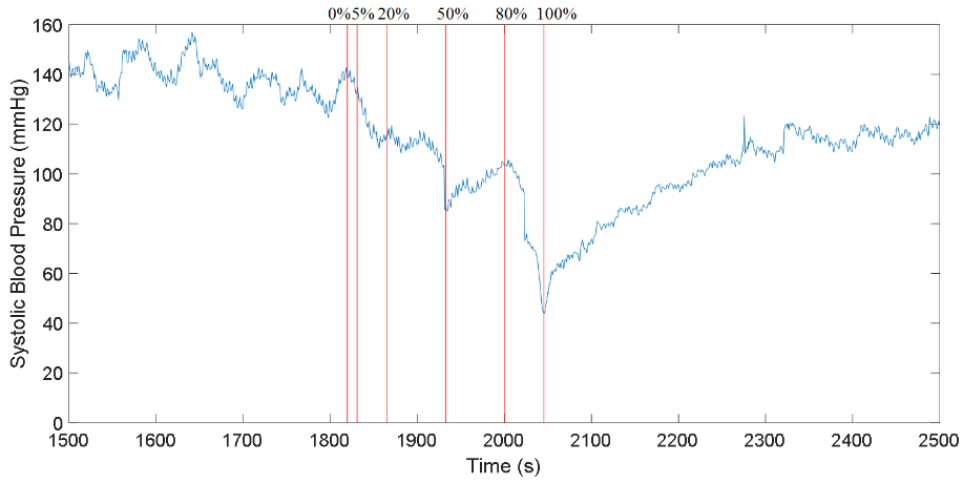

Figure 31 – Representation of the reference values used to the extraction of PAT values (0%, 5%, 20%, 50%, 80% and 100%), from the moment that Systolic Blood Pressure starts to decrease (0%) until the SBP minimum peak (100%). Based on [1].

5.3. Results and Discussion

5.3.1. Implemented Algorithm for Pulse Presence Classification

Regarding the cut-off frequency, according to Figure 32 and Table VI, the optimal one that should be used to improve the performance of the present algorithm is 5 Hz. Although, for other frequencies within a certain range (2.5Hz-6Hz), the results were also very similar. Consequently, all results and conclusions presented in the reaming of this chapter are associated to a high-pass filter applied to the ACC signal with a cut-off frequency of 5 Hz.

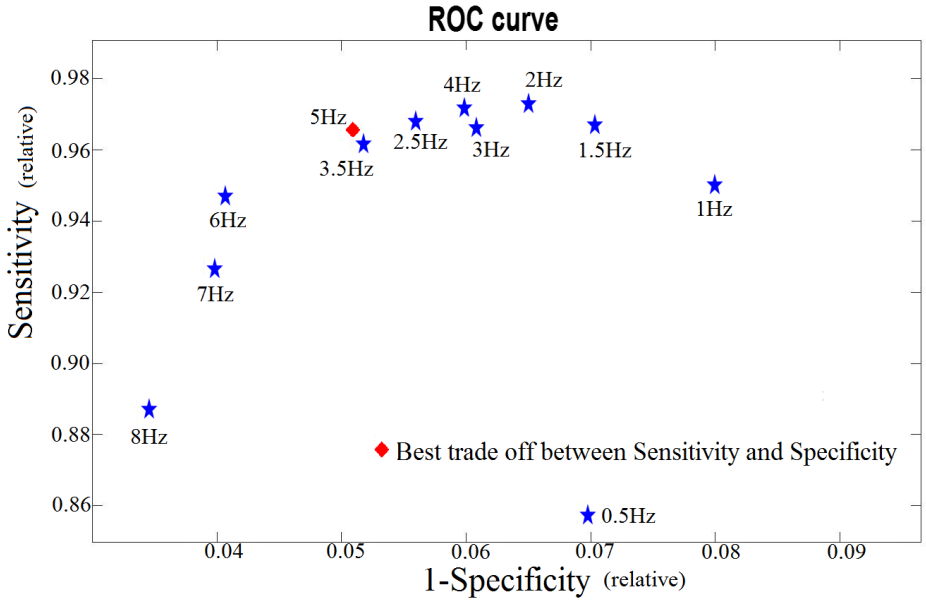

Figure 32 - Different performances associated to the change of the cut-off frequency of the ACC high-pass filter.

Table VI – Performance of the algorithm for the different cut-off frequencies (fc) of the ACC high-pass filter.

FC (HZ)	0.5	1.00	1.50	2.00	2.50	3	3.5	4	5	6	7	8
SEN (%)	85.7	95.0	96.7	97.3	96.8	96.6	96.3	97.1	96.6	94.6	92.7	88.7
SPE (%)	93.0	92.0	92.0	93.5	94.4	93.9	94.9	94.0	94.9	96.0	96.0	96.5

Table VII shows the level of the ACC artifacts contamination of each patient identified by the noise classifier. As can be observed, the level of contamination was relatively small for most of the patients, but not for patients 5 and 7. A large portion of the acquired signals was lost for these two patients.

Table VII - Level of contamination identified on the ACC signal by the noise classifier for each patient.

	CONTAMINATION LEVEL
PATIENT 1	6.7%
PATIENT 2	15.8%
PATIENT 3	6.5%
PATIENT 4	3.6%
PATIENT 5	37.1%
PATIENT 6	8.5%
PATIENT 7	44.8%
PATIENT 8	7.8%

Table. VIII summarizes the average performance of the algorithm, evaluated with the test group, using the optimal threshold determined from the training data set. It was found very promising results, with SEN of 96.6% and SPE of 94.9% for this initial implementation.

Table VIII - Performance of the algorithm and global results (entire dataset-8 patients; fc=5Hz; L=20%).

	TEST GROUP	GLOBAL
SEN (%)	96.6	94.5
SPE (%)	94.9	94.3

In Table IX it is presented the results per patient using the best threshold to identify possible outliers as well as to verify if the performance of the algorithm in the referenced patients (2, 5, 6, 7 and 8) has been affected. For patient 2 and patient 5 the achieved sensitivity values were lower compared to the results for the other patients. The sensitivity for patient 5 is even lower than for patient 2. In the case of patient 8, the performance was good with SEN and SPE above 90%. This may have been due to the fact that, for pulse classification, the correlation between ACC and ECG was not significantly affected by PVCs. Regarding patients 6 and 7, the performance was also considerably good. This may suggest that despite the strange morphology that both signals had (see Figure 22), the algorithm was able to classify the pulse presence accurately.

Table IX - Sensitivity and specificity for each patient when the optimal threshold was used.

PATIENT	**1**	**2**	**3**	**4**	**5**	**6**	**7**	**8**
SEN (%)	99.6	86.1	98.3	98.6	60.8	94.8	99.4	92.3
SPE (%)	95.1	92.4	94.3	89.5	98.0	95.2	93.8	95.8

The correlation coefficients of patient 5 shown in Figure 28 (bottom) exhibit a low contrast for phases of pulse absence versus phases with pulse presence. Also, it was observed large variations in the correlation coefficients, which might be caused by the

powerline interference in the ECG, as well as a low SNR of the ACC signal, as can be observed in Figure 33. This leads to a weak separation of pulse presence versus absence, being difficult to discriminate them solely using a simple thresholding approach. Hence a significant misclassification was obtained for patient 5. The same situation has happened with patient 2 due to the low quality of the signal.

For ACC signals with a high SNR making a pulse easily observable, the correlation coefficient seams very well determined and able to separate phases of pulse presence versus pulse absence reliably. This is illustrated in Figure 28 (top) where periods without pulse have a correlation coefficient lower than 0.2, and where phases with pulse typically have a higher correlation coefficient.

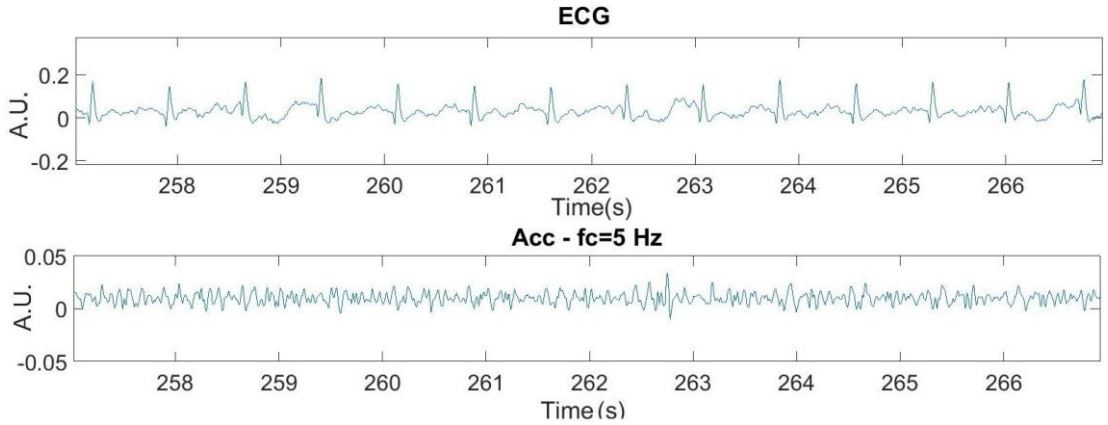

Figure 33 - Examples of Signals of Patient 5: (top) Filtered ECG; (bottom) filtered ACC fc=5Hz.

5.3.2. Implemented Algorithm for Pulse Arrival Time extraction

According to [37], PAT is influenced by the Pre-ejection Period and Pulse Transit Time. Regarding PTT, it has been subject to special interest in the medical and biomedical literature, due to its strong dependence on physiological variables such as peripheral resistance, arterial compliance and blood pressure [35]. Thus, assuming a constant PEP and taking into account that PAT=PEP+PTT, as referred in chapter3, it is expected that an increase of SBP be reflected in a decrease of PTT, which consequently is reflected on a decrease of PAT. On the other hand, a decrease of SBP leads to an increase of PTT, and subsequently to an increase of PAT.

Therefore, since syncope event is identified in this case by an abrupt decrease in SBP, it should correspond to an abrupt increase of PAT.

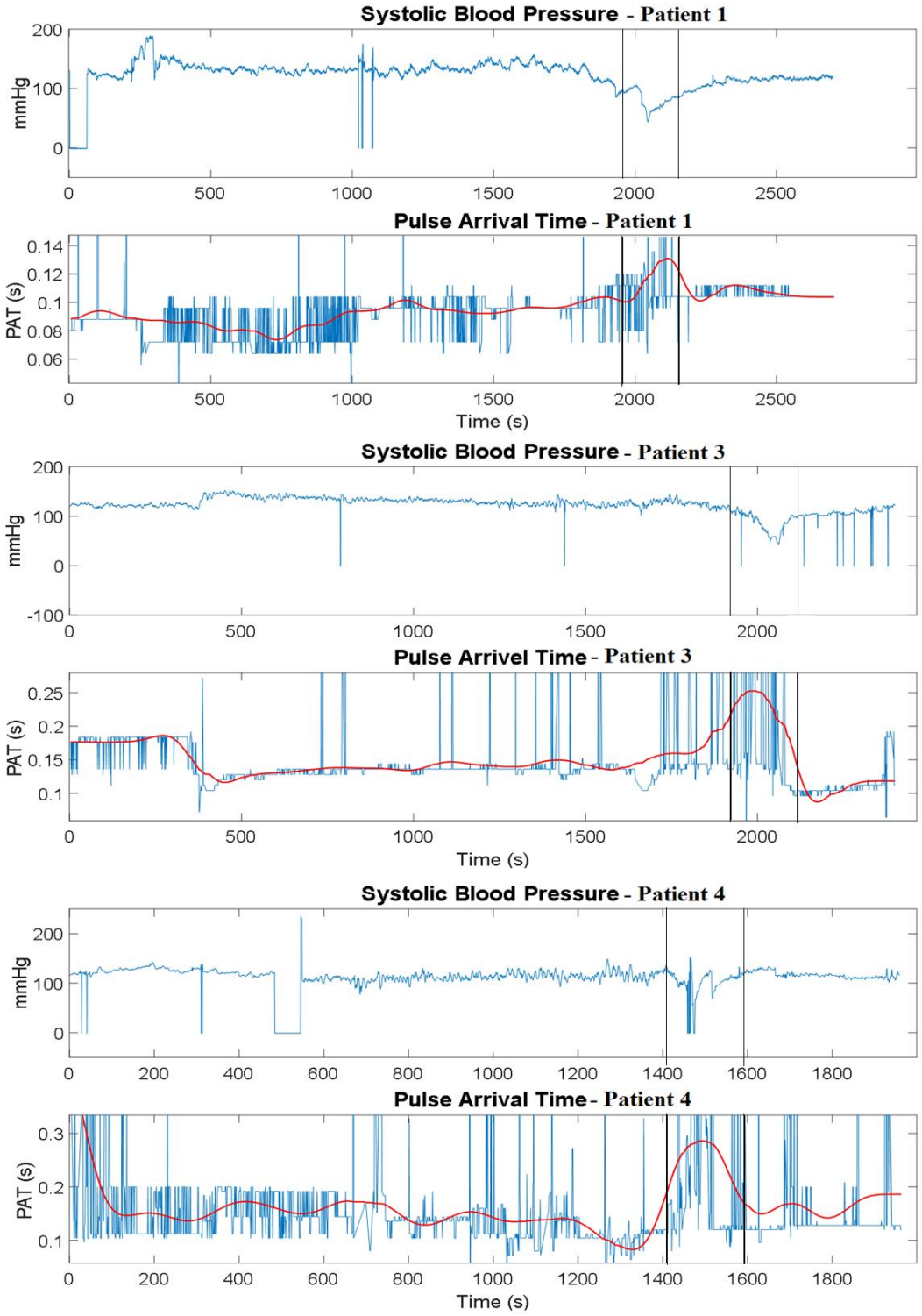

Figure 34 – Representation of Systolic Blood Pressure and Pulse Arrival Time evolution for patient 1, 3 and 4. The region comprehended between the black vertical lines, defines the region of syncope (the blue and red signals correspond to the PAT before and after being filtered respectively).

In Figure 34 the SBP and the extracted PAT are represented for patients 1, 3 and 4. Focusing just on the red signals, it is observed that the PAT variations followed the

expectations. Within certain limits of oscillations, for the 3 patients, the PAT remained relatively constant until the region where blood pressure regulation started to fail. Here, SBP began to decrease, which has disturbed the PAT levels significantly, with a considerable increase of its values. After SBP had returned to normal values (spontaneous recovery of the patient), the PAT decreased, stabilizing. Thus, for these patients, visually the variations of PAT were as expected.

For the further analysis, only the mentioned 3 patients (patient 1, patient 3 and patient 4) were considered. This was due to the fact that patient 7 and 8 did not suffer any syncope event (the SBP remained stable) and patient 2, 5 and 6 had a very questionable ACC and/or ECG signal quality. The PAT was very unstable with a very high number of outliers, not allowing any conclusions to be drawn about them (see Figure 35). Concerning patient 6, despite the good results achieved on the pulse presence classifier, the morphology proved to be a crucial parameter for a reliable PAT extraction using this approach (see Figure 22).

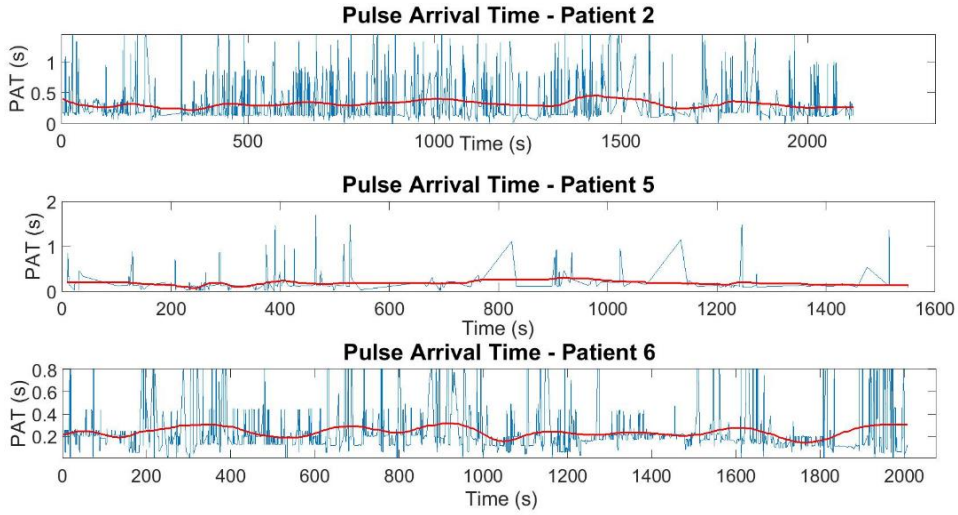

Figure 35 – Representation of Pulse Arrival Time evolution for patient 2, 5 and 6 (the blue and red signals correspond to the PAT before and after being filtered respectively).

Regarding the cross-correlation procedure, it was applied between a specific interval of the SBP and PAT signals. The interval was defined between 3 minutes before the SBP minimum peak until the minimum peak. Thereby, according to Table X, for all patients the correlation coefficient was negative, as it was predicted. Although, the absolute values were significantly low, having an average of 0.44 for the three patients. This can be, mainly due to the delay imposed to PAT at the moment of extraction by the 3 seconds correlation window, as mentioned before.

Table X – Correlation coefficient between PAT and SBP, since 3 minutes before the SBP minimum peak until the minimum peak.

	PATIENT 1	PATIENT 3	PATIENT 4
CORRELATION COEFFICIENT	-0.64	-0.32	-0.36
MEAN		-0.44	

Therefore, another correlation process was made considering a delay between both signals, in order to find the optimal correlation position.

Table XI - Correlation coefficient between PAT and SBP with delay tolerated, since 3 minutes before the SBP minimum peak until the minimum peak (Optimal delay <0 PAT anticipates SBP; Optimal delay>0 SBP anticipates PAT).

	PATIENT 1	PATIENT 3	PATIENT 4
CORRELATION COEFFICIENT	-0.65	-0.91	-0.57
OPTIMAL DELAY (s)	-10	-86	-59
MEAN		-0.71	

In this way, Table XI represents the optimal correlation coefficients, and respective delay between PAT and SBP. The correlation coefficients remained negative, with an absolute value much higher than the previous one, with an average of 0.71. This confirms the inverse relation that characterizes both signals.

Despite the good results, PAT extraction method just justifies possible delays around 3 seconds, as mentioned. These delays, were much higher. The main cause of this delay is the number of outliers in the region (see Figure 34). This method of PAT extraction is very sensitive to the signals' morphology (ACC and ECG). Any kind of variation in morphology, even the smallest one, can influence and be reflected in a PAT change. As Figure 36 depicts, the morphology change verified on the first pulse, was enough to create an outlier. This could be an advantage in the way that increases the accuracy of the method, but on the other hand, makes it very susceptible to contaminations and outliers.

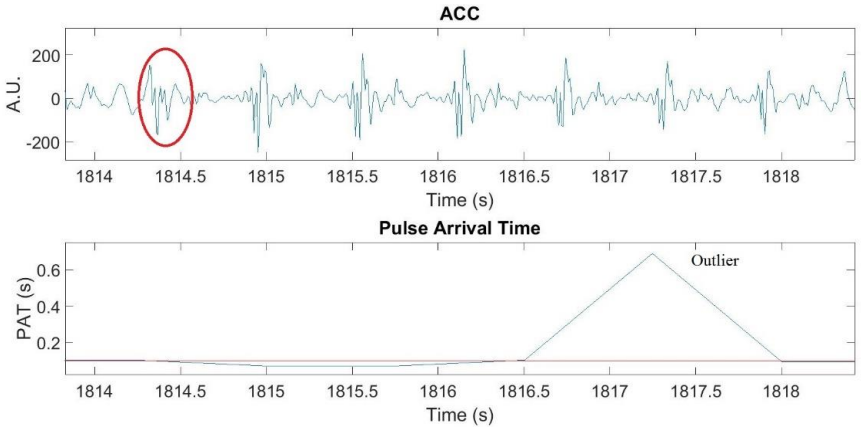

Figure 36 – Representation of the influence of the signal morphology in PAT extraction. Example of an outlier cause. Red circle shows the change of morphology in an ACC signal.

As can be observed in Figure 37, when the SBP began to decrease, the ACC quality worsened, which led to a large increase in the number of outliers in the syncope region. In this phase the patient tends to move a lot, compromising the best match between PAT and SBP.

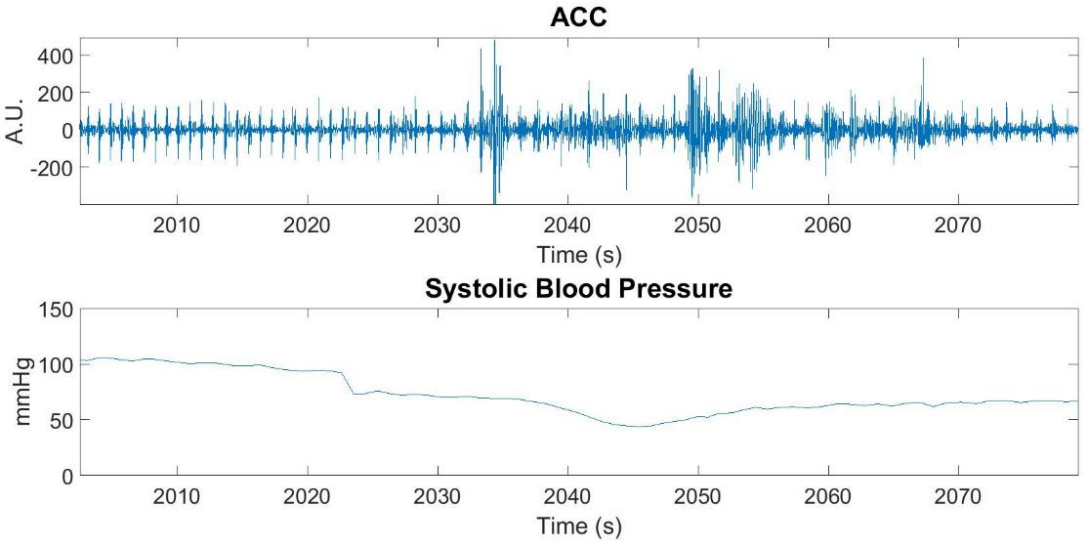

Figure 37 – Representation of the noise of the ACC signal that characterizes the syncope region.

Concerning the extraction of PAT reference values, since the moment that SBP started to decrease ($PAT_{0\%}$) until the SBP reaches the minimum peak ($PAT_{100\%}$), the results were as expected. As can be observed in Table XII, for all of the 3 patients under analysis, there is a growing trend from $PAT_{0\%}$ to $PAT_{100\%}$. Comparing with respect to PAT_{REF}, patient 1 shows an increase of 37%, patient 3 of 73% and in patient 4 shows also an increase of 109%.

Table XII - Reference values used to the extraction of PAT values (0%, 5%, 20%, 50%, 80% and 100%), from the moment that Systolic Blood Pressure starts to decrease (0%) until the occurrence of syncope event (100%). All the values were normalized by PAT_{REF}.

	PATIENT 1	**PATIENT 3**	**PATIENT 4**
PAT_{REF}	**0.09**	**0.12**	**0.13**
PAT	**Relative values**		
$PAT_{0\%}$	1.17	1.83	1.46
$PAT_{5\%}$	1.18	1.90	1.52
$PAT_{20\%}$	1.20	2.05	1.68
$PAT_{50\%}$	1.19	2.12	1.93
$PAT_{80\%}$	1.21	1.98	2.06
$PAT_{100\%}$	1.37	1.73	2.09

Therefore, all the results presented, reinforce the idea that PAT and the SBP vary in a completely opposite way, verifying an evident increase of PAT during a syncope event.

5.4. Conclusion and Future Work

In this chapter it was introduced a simple algorithm based on a signal fusion approach of synchronously acquired ECG and ACC signals to discriminate pulse presence/pulse absence and to further assess ACC-based PAT as a BP surrogate.

The proposed method for pulse presence classification is simple and can be easily implemented in devices with low processing power: a similarity metric based on a simple linear correlation coefficient seems to provide a reasonable feature for pulse presence detection. A simple threshold-based classifier is applied to discriminate pulse presence/absence. Although the presented results have been assessed on a small database, these initial results are promising, with sensitivity and specificity above 90%, since it was found consistent performance even for patients with severe arrhythmia. It was evident the difference from segments with/without pulse presence, showing in the case of absence, considerably lower correlation coefficients.

Regarding the method for PAT inference, it is also very simple to apply. Despite the good results for 3 patients, showing an evident correlation between SBP and PAT, the method proved to be very sensitive to any kind of contamination that the ACC or ECG signal may exhibit. This compromises the viability of this approach to use the accelerometer sensor as a wearable, once it is very susceptible to movement artifacts. Therefore, the next steps should be to evaluate these results using an extended database. A correlation between the PAT extracted from this method and PAT inferred between ECG and PPG should also be of interest, in order to verify/reinforce the conclusions drawn in here.

Chapter 6

Conclusions and Future Work

The thesis explored the potential use of an ACC sensor placed over the carotid to accurately detect and characterize the carotid pulse as a means to develop syncope detection solutions as well solutions to support CPR. Regarding syncope, due to its huge impact on healthcare costs and in the quality of life, especially in elderly people, it was found a priority to find a continuous monitoring mechanism that was able to anticipate and predict a syncope event. Such a solution would allow people to take countermeasures in an eminent situation, preventing most part of syncope events. Cardiopulmonary resuscitation was also another area of interest due to the limitations of current approaches for pulse detection which are unreliable and error prone. Taking into consideration that the efficiency and responsiveness of the resuscitation process is preponderant for successful rescue, a reliable and automatic pulse detection technique should also be a priority.

Despite their potential, accelerometers are very susceptible to movement artifacts. Therefore, as a first challenge, it was designed an algorithm to handle with those artifacts properly. It was investigated the application of low complexity energy features (mean, variance, 3^{rd} and 4^{th} statistical moments and teager energy) in the detection of those contaminations. A simple threshold-based was applied to discriminate noise/no noise in healthy subjects. It is shown that very promising results can be achieved with a simple feature as the first statistical moment of the signal energy, with sensitivity and specificity above 90%. A complementarity between the first and the third statistical moments, should also be interesting for the elaboration of a more robust multi-feature classifier.

The second challenge, after the noise classifier, was to develop a simple algorithm based on a signal fusion approach of synchronously acquired ECG and ACC signals to discriminate pulse presence/pulse absence and to assess whether ACC-based PAT inference might be used as a BP surrogate. The proposed method for pulse presence classification and PAT inference is based on a simple linear correlation features, between ECG and ACC signal, applied on a small database of patients submitted to HUTT test. For the pulse presence the amplitude of the maximum cross-correlation coefficient was

used and for the ACC-based PAT inference the lag relative to the aforementioned maximum was considered. A simple threshold-based classifier was applied to discriminate pulse presence/absence, achieving promising results, with sensitivity and specificity above 90%, even for compromised patients with severe arrhythmia. It was evident the difference from segments with/without pulse presence, showing in the case of absence, considerably lower correlation coefficients.

Concerning the method for PAT inference, applied in a problematic database, with patients with poor quality signals, it proved to be very sensitive to any kind of contamination or morphology interference that ACC or ECG signals may exhibit. It showed to be adequate in just 3 of the 8 available patients in this study. The results associated to these patients were promising showing an evident negative correlation between SBP and PAT. Despite the good results for the aforementioned patients, this approach appeared to be highly susceptible to contaminations for PAT extraction, compromising the usability of this feature as a blood pressure surrogate.

The limitations of a reduced database for both methods, do not enable to draw any kind of definitive conclusions or to perform any kind of generalization. In this way, the conditions imposed, namely the noise threshold and the pulse presence threshold used, might easily change once an extended or different dataset is applied. Consequently, the presented results in this thesis should be read with care. In spite of this, the methodologies developed and tested, revealed optimistic results. Therefore, regarding the first challenge, the next step would be to apply it in a more extensive dataset collected using an adequate target population, to assess of the ACC signal quality in terms of diagnostic value during artifact contamination and to explore disturbance of the quasi-periodic nature of pressure pulses in order to detect artifacts. With regard to the seconds challenge, the next steps necessarily comprise the extension of the available database in order to generalize both methods applied. A correlation between the PAT extracted from this method and PAT inferred between ECG and PPG should also be interesting to do, in order to verify/reinforce the conclusions obtained.

Given this, despite the heterogeneity of the achieved results and considering the limitation imposed by the small database available for this study, it is safe to say that the main goals of the thesis to contribute with new useful knowledge for the innovation CPR and syncope prediction mechanisms have been accomplished.

References

[1] R. Couceiro *et al.*, “Characterization of Surrogate Parameters for Blood Pressure Regulation in Neurally - Mediated Syncope,” pp. 3–7, 2013.

[2] A. Moya *et al.*, “Guidelines for the diagnosis and management of syncope (version 2009),” *Eur. Heart J.*, vol. 30, no. 21, pp. 2631–2671, 2009.

[3] N. Colman *et al.*, “Epidemiology of reflex syncope,” *Clin. Auton. Res.*, vol. 14, no. SUPPL. 1, pp. 9–17, 2004.

[4] D. M. Lemonick, “Evaluation of Syncope in the Emergency Department,” vol. 16, no. 3, pp. 11–19, 2010.

[5] A. Alshekhlee, W.-K. Shen, J. Mackall, and T. C. Chelimsky, “Incidence and mortality rates of syncope in the United States.,” *Am. J. Med.*, vol. 122, no. 2, pp. 181–8, 2009.

[6] M. P. Tan and R. A. Kenny, “Cardiovascular assessment of falls in older people.,” *Clin. Interv. Aging*, vol. 1, no. 1, pp. 57–66, 2006.

[7] C. Kessler, J. M. Tristano, and R. De Lorenzo, “The Emergency Department Approach to Syncope: Evidence-based Guidelines and Prediction Rules,” *Emerg. Med. Clin. North Am.*, vol. 28, no. 3, pp. 487–500, 2010.

[8] J. C. Jentzer, C. M. Clements, J. G. Murphy, and R. Scott Wright, “Recent developments in the management of patients resuscitated from cardiac arrest,” *J. Crit. Care*, vol. 39, pp. 97–107, 2017.

[9] F. Adnet *et al.*, “Cardiopulmonary resuscitation duration and survival in out-of-hospital cardiac arrest patients,” *RESUS Resusc.*, vol. 7003, pp. 1–8, 2016.

[10] K. Dellimore *et al.*, “Towards an algorithm for automatic accelerometer-based pulse presence detection during cardiopulmonary resuscitation,” 2016.

[11] C. D. Deakin and J. L. Low, “Accuracy of the advanced trauma life support guidelines for predicting systolic blood pressure using carotid, femoral, and radial pulses: observational study.,” *BMJ*, vol. 321, no. 7262, pp. 673–4, Sep. 2000.

[12] S. Brearley, C. P. Shearman, and M. H. Simms, “Peripheral pulse palpation: an

unreliable physical sign.," *Ann. R. Coll. Surg. Engl.*, vol. 74, no. 3, pp. 169–71, May 1992.

[13] M. Lundin *et al.*, "Distal Pulse Palpation: Is It Reliable?," *World J. Surg.*, vol. 23, no. 3, pp. 252–255, Mar. 1999.

[14] B. Eberle, W. F. Dick, T. Schneider, G. Wisser, S. Doetsch, and I. Tzanova, "Checking the carotid pulse check: diagnostic accuracy of first responders in patients with and without a pulse," *Resuscitation*, vol. 33, no. 2, pp. 107–116, Dec. 1996.

[15] F. J. Ochoa, E. Ramalle-Gómara, J. . Carpintero, A. García, and I. Saralegui, "Competence of health professionals to check the carotid pulse," *Resuscitation*, vol. 37, no. 3, pp. 173–175, Jun. 1998.

[16] J. Muehlsteff, K. Dellimore, V. Aarts, R. Derkx, C. Peiker, and C. Meyer, "Pulse detection with a single accelerometer placed at the carotid artery: Performance in a real-life diagnostic test during acute hypotension," in *2015 37th Annual International Conference of the IEEE Engineering in Medicine and Biology Society (EMBC)*, 2015, pp. 434–437.

[17] Sylvia S.Mader, *Understanding Human Anatomy And Physiology (5 Ed, 2004) Mader : Sylvia Mader : Free Download & Streaming : Internet Archive*, 5th ed. 2004.

[18] G. J. Tortora and B. Derrickson, *Principles Of Anatomy And Physiology 12th Ed G. Tortora, B : Free Download & Streaming : Internet Archive*, 12th ed. 2009.

[19] C. B. Munjewar, "Structure of Heart & Circulation," *The Fit Heart*, 2017. [Online]. Available: http://www.www.thefitheart.in/structure-of-heart. [Accessed: 16-Aug-2017].

[20] J. R. Weber and J. H. Kelley, *Health Assessment in Nursing*, 5th ed. .

[21] "Cardiac Cycle · Anatomy and Physiology, OpenStax College." [Online]. Available: http://philschatz.com/anatomy-book/contents/m46661.html. [Accessed: 09-Aug-2017].

[22] J. R. Levick, *An introduction to cardiovascular physiology*. 1991.

[23] R. E. Klabunde, *Cardiovascular Physiology Concepts*, 2nd ed. 2011.

[24] W. Wieling, R. D. Thijs, N. Van Dijk, A. A. M. Wilde, D. G. Benditt, and J. G. Van Dijk, "Symptoms and signs of syncope: A review of the link between physiology and clinical clues," *Brain*, vol. 132, no. 10, pp. 2630–2642, 2009.

[25] T. D. Rea *et al.*, "CPR with Chest Compression Alone or with Rescue Breathing," *N. Engl. J. Med.*, vol. 363, no. 5, pp. 423–433, Jul. 2010.

[26] J. P. Ornato and M. ann Peberdy, *Cardiopulmonary Resuscitation*. 2005.

[27] B. B. Graham, *Using an Accelerometer Sensor to Measure Human Hand Motion*, submitted to the Department of Electrical Engineering and Computer Science in Partial Fulfillment of the Requirements for the Degrees of Bachelor of Science in Electrical Science and Engineering and Master of Engineering in Eletrical Engineering and Computer Science, Massachusetts Institute of Teechnology. 2000.

[28] J. Muehlsteff *et al.*, "Feasibility of pulse presence and pulse strength assessment during head-up tilt table testing using an accelerometer located at the carotid artery," *Conf. Proc. ... Annu. Int. Conf. IEEE Eng. Med. Biol. Soc. IEEE Eng. Med. Biol. Soc. Annu. Conf.*, vol. 2014, pp. 894–897, 2014.

[29] V. T. van Hees *et al.*, "Separating Movement and Gravity Components in an Acceleration Signal and Implications for the Assessment of Human Daily Physical Activity," *PLoS One*, vol. 8, no. 4, pp. 1–10, 2013.

[30] L. Giovangrandi, O. T. Inan, R. M. Wiard, M. Etemadi, and G. T. A. Kovacs, "Ballistocardiography - A method worth revisiting," *Proc. Annu. Int. Conf. IEEE Eng. Med. Biol. Soc. EMBS*, pp. 4279–4282, 2011.

[31] D. B. Rendón, J. L. Rojas Ojeda, L. F. Crespo Foix, D. S. Morillo, and M. A. Fernández, "Mapping the human body for vibrations using an accelerometer.," *Conf. Proc. ... Annu. Int. Conf. IEEE Eng. Med. Biol. Soc. IEEE Eng. Med. Biol. Soc. Annu. Conf.*, vol. 2007, pp. 1671–4, 2007.

[32] N. H. P. M. Pinheiro, Master Thesis: *iLook Over You*., University of Coimbra, Coimbra 2017.

[33] M. Elgendi, "On the analysis of fingertip photoplethysmogram signals.," *Curr.*

Cardiol. Rev., vol. 8, no. 1, pp. 14–25, 2012.

[34] M. Roos, S. Toggweiler, M. Zuber, P. Jamshidi, and P. Erne, "Acoustic cardiographic parameters and their relationship to invasive hemodynamic measurements in patients with left ventricular systolic dysfunction.," *Congest. Heart Fail.*, vol. 12 Suppl 1, no. august, pp. 19–24, 2006.

[35] P. Carvalho, "Assessing Cardiovascular Status for pHealth Applications." (private communication).

[36] J. Muehlsteff *et al.*, "Pulse arrival time as surrogate for systolic blood pressure changes during impending neurally mediated syncope," *Proc. Annu. Int. Conf. IEEE Eng. Med. Biol. Soc. EMBS*, pp. 4283–4286, 2012.

[37] R. Couceiro, PhD Thesis: *Cardiovascular Performance Assessment for P - Health Applications*, University of Coimbra, Coimbra, 2014.

[38] P. Shaltis, A. Reisner, and H. Asada, "A hydrostatic pressure approach to cuffless blood pressure monitoring.," *Conf. Proc. IEEE Eng. Med. Biol. Soc.*, vol. 3, no. 4, pp. 2173–6, 2004.

[39] J. Beckerman, "Heart Disease and the Head-Up Tilt Table Test," *© 2016 WebMD, LLC*. [Online]. Available: http://www.webmd.com/heart-disease/guide/tilt-table-test#1. [Accessed: 19-Aug-2017].

[40] N. Virag, R. Sutton, R. Vetter, T. Markowitz, and M. Erickson, "Prediction of vasovagal syncope from heart rate and blood pressure trend and variability: Experience in 1,155 patients," *Hear. Rhythm*, vol. 4, no. 11, pp. 1375–1382, 2007.

[41] R. Mereu, G. De Barbieri, T. Perrone, A. Mugellini, A. Di Toro, and L. Bernardi, "Heart rate/blood pressure ratio as predictor of neuromediated syncope," *Int. J. Cardiol.*, vol. 167, no. 4, pp. 1170–1175, 2013.

[42] J. Muehlsteff *et al.*, "Detection of hemodynamic adaptations during impending syncope: Implementation of a robust algorithm based on pulse arrival time measurements only," *Proc. Annu. Int. Conf. IEEE Eng. Med. Biol. Soc. EMBS*, pp. 2291–2294, 2013.

[43] R. Couceiro *et al.*, "Real-Time Prediction of Neurally Mediated Syncope," *IEEE J. Biomed. Heal. INFORMATICS, VOL.00, NO 00, 2015*.

[44] R. Couceiro *et al.*, “Algorithm for Real-time Prediction of Neurally Mediated Syncope Integrating Indexes of Autonomic Modulation,” pp. 685–688, 2015.

[45] L. Mason, “Signal processing methods for non-invasive respiration monitoring,” *Philosophy*, p. 175, 2002.

[46] D. H. Phan, S. Bonnet, R. Guillemaud, E. Castelli, and N. Y. Pham Thi, “Estimation of respiratory waveform and heart rate using an accelerometer.,” *Annu. Int. Conf. IEEE Eng. Med. Biol. Soc.*, vol. 2008, pp. 4916–9, 2008.

[47] D. S. Morillo, J. L. Rojas Ojeda, L. F. Crespo Foix, D. Barbosa Rendón, and A. León, “Monitoring and analysis of cardio respiratory and snoring signals by using an accelerometer,” *Annu. Int. Conf. IEEE Eng. Med. Biol. - Proc.*, pp. 3942–3945, 2007.

[48] M. Jaeger *et al.*, “First-aid sensor system: New methods for single-point detection and analysis of vital parameters such as pulse and respiration,” *Annu. Int. Conf. IEEE Eng. Med. Biol. - Proc.*, pp. 2928–2931, 2007.

[49] R. W. C. G. R. Wijshoff *et al.*, “Detection of a spontaneous pulse in photoplethysmograms during automated cardiopulmonary resuscitation in a porcine model,” *Resuscitation*, vol. 84, no. 11, pp. 1625–1632, 2013.

[50] P. Hubner, J. Muehlsteff, R. Wijshoff, J. K. Russell, K. Nammi, and F. Sterz, “Pulse appearance in photoplethysmography signals obtained from finger, nose and ear during extracorporeal life support,” *Resuscitation*, vol. 96, p. 44, 2015.

[51] N. L. Rollinson, “Understanding and Managing Neurally Mediated Syncope in the Adolescent,” *J. Sch. Nurs.*, vol. 21, no. 4, pp. 200–207, Aug. 2005.

[52] M. Anpalahan, “Neurally mediated syncope and unexplained or nonaccidental falls in the elderly,” *Intern. Med. J.*, vol. 36, no. 3, pp. 202–207, Mar. 2006.

[53] J. J. Seger, “Syncope evaluation and management.,” *Texas Hear. Inst. J.*, vol. 32, no. 2, pp. 204–6, 2005.

[54] A.-M. Tautan, A. Young, E. Wentink, and F. Wieringa, “Characterization and reduction of motion artifacts in photoplethysmographic signals from a wrist-worn device,” in *2015 37th Annual International Conference of the IEEE Engineering in Medicine and Biology Society (EMBC)*, 2015, vol. 2015, pp. 6146–6149.

[55] R. W. C. G. R. Wijshoff, M. Mischi, and R. M. Aarts, “Reduction of Periodic Motion Artifacts in Photoplethysmography,” *IEEE Trans. Biomed. Eng.*, vol. 64, no. 1, pp. 196–207, Jan. 2017.

[56] R. Mooney, G. Corley, A. Godfrey, L. R. Quinlan, and G. ÓLaighin, “Inertial Sensor Technology for Elite Swimming Performance Analysis: A Systematic Review.,” *Sensors (Basel).*, vol. 16, no. 1, Dec. 2015.

[57] J. Muehlsteff, P. Carvalho, J. Henriques, R. P. Paiva, and H. Reiter, “Cardiac status assessment with a multi-signal device for improved home-based congestive heart failure management,” in *2011 Annual International Conference of the IEEE Engineering in Medicine and Biology Society*, 2011, vol. 2011, pp. 876–879.

[58] “All About Heart Rate (Pulse),” *American Heart Association*, 2015. [Online]. Available: http://www.heart.org/HEARTORG/Conditions/More/MyHeartandStrokeNews/All-About-Heart-Rate-Pulse_UCM_438850_Article.jsp#.WZb3jj4jFaR. [Accessed: 18-Aug-2017].

[59] P. A. Meaney *et al.*, “Cardiopulmonary resuscitation quality: Improving cardiac resuscitation outcomes both inside and outside the hospital: A consensus statement from the American heart association,” *Circulation*, vol. 128, no. 4, pp. 417–435, 2013.

[60] “Singular Value Decomposition (SVD).” [Online]. Available: https://www.cs.cmu.edu/~venkatg/teaching/CStheory-infoage/book-chapter-4.pdf. [Accessed: 17-Aug-2017].

[61] L. Wei, T. Yu, P. Gao, W. Quan, Y. Li, “Detection of Spontaneous Pulse Using Acceleration Signals Acquired From CPR Feedback Sensor in Porcine Model of Cardiac Arrest” Circulation, Volume 134.

Appendices

Appendix A

"Artifact detection in Accelerometer Signals acquired from the Carotid"

Scientific publication presented at the 39th Annual International Conference of the Engineering in Medicine and Biology Society (EMBC' 17) of the Institute for Electrical and Electronics Engineers (IEEE), Seoul, South Korea, 2017. Authors: B. Silva, J. Muehlsteff, R. Couceiro, J. Henriques and P. Carvalho.

Artifact detection in Accelerometer Signals acquired from the Carotid

B. Silva, J. Muehlsteff, R. Couceiro, J. Henriques, P. Carvalho

Abstract — **Manual pulse palpation is the common procedure to assess pulse in unconscious patients. This is an error prone procedure during cardiopulmonary resuscitation and therefore automatic pulse detection techniques are being investigated. Accelerometry is an interesting sensing modality for this type of applications. However, accelerometers are highly prone to movement artifacts. Hence, one challenge in designing a solution using accelerometers is to handle motion artifacts properly. In this paper we investigate computationally simple features and classifier to capture movement artifacts in accelerometer signals acquired from the carotid. In particular, based on data obtained from health subjects we show that it is possible to use simple features to achieve an artifact detection sensitivity and specificity higher than 90%.**

I. INTRODUCTION

Manual palpation is still the most basic approach to check for pulse presence in an unconscious patient. It is also used for easy to perform pulse rate measurements e.g. in low acuity settings or after a physical exercise. The procedure consists of placing a finger above an artery close to the skin surface such as the carotid, femoral or radial artery and to feel the pulsations. Presence or absence of a palpable pulse also provides a rough estimate of the systolic blood pressure (SBP) [1], e.g. in case the pulse can be felt at the carotid only, SBP is assumed to be approximately 60 mmHg. However, palpation which is still the "Golden reference" for pulse check has been shown to be error prone and often takes too long during cardiopulmonary resuscitation (CPR) [2-5]. Therefore, palpation-based pulse checks by layman are not recommended anymore in emergency care guidelines. Due to this fact, there is a need for a sensing modality, which is 1.) easy to apply in demanding stressful situations, 2) can objectify and preferably quantify pulse presence and 3) can be understood by consumers for acceptance.

An interesting sensing modality for this problem are accelerometer (ACC), which have found widespread use in many consumer applications in particular in Smartphones, tablets but also wrist-worn watches. Low cost, low power, small and inexpensive sensors with high sensitivities are available. They enable sophisticated signal processing techniques e.g. for noise and artifact reduction via signal fusion techniques [6,7], for motion detection and classification e.g. in sport such as swimming [8] but also for vital sign and context measurements. Also, ACC sensors allow electrode-free monitoring with sufficient performance for monitoring of mobile patients in general for which a FDA approved cableless sensor embodiment is commercially available [9]. An ACC sensor may provide a means of objectifying pulse palpation, which has been demonstrated in our previous work on the basic feasibility of ACC-based pulse detection from signals acquired from the carotid artery [10-12]. The aim of this study is to extend insights in more sophisticated artifact handling using this approach.

The ACC signal is prone to various sources of error (e.g., motion artifacts), which can complicate the extraction of reliable vital sign parameters and compromise the utility of the ACC in healthcare applications. Thereby, it is very important to detect those sections of the signal, which are contaminated by artifacts in order to leave these periods out for vital sign extractions. In this paper, our goal is to assess the ability of different simple features to capture these artifacts in ACC signals obtained at the carotid. We introduce a systematic analysis of the detection performance based on low computational complexity features that can be easily integrated into embedded systems as required in portable pHealth applications as well as in resuscitation systems. A simple threshold-based classifier is proposed to detect artifacts in ACC signals collected from the carotid.

II. METHODS

A. Experimental Protocol and Setup

To develop and test our methodology, a data collection study was performed with 12 healthy volunteers. The protocol was designed to capture typical artifacts to be expected during daily life activities (e.g., head and neck movements, talking, swallowing, etc.), but also extreme situations such as jumping (simulation of rapid body movements). Specifically, the protocol consisted of four phases without any noise (two in the supine and two in the seated positions), and six phases characterized by a specific movement such as: arm movements in the horizontal position, speech, rotation of the neck, moving from sitting to the standing up position, swallowing and jumping. Each of these phases had a duration of 20 seconds and were separated from each other by a transition phase of 10 seconds. The acquisition process for each subject has a total duration of 300 seconds (5 minutes) as illustrated in Fig.1. The Data was recorded from twelve healthy volunteers that provided informed consent. The age of the participant group

This work was supported by project LINK (H2020 – 692023). B. Silva, J. Henriques and P. Carvalho are with CISUC, Department of Informatics Engineering, University of Coimbra, Portugal (e-mail: bernardosilva1694@gmail.com, {rcouceir, jh, carvalho,} @dei.uc.pt).

J. Muehlsteff is with Philips Research, Eindhoven, The Netherlands (email: jens.muehlsteff@philips.com).

was 29±11 (mean ± SD) years (from 22 to 49 years) and body mass index (BMI) was 23.28±2.02 kg.m^{-2} (mean ± SD).

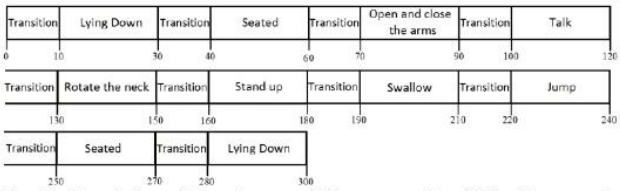

Fig. 1- Description of the data acquisition protocol activities/phases and respective duration (seconds).

The accelerometer signals were acquired from the common carotid with a multi-parameter, battery operated device called "SENSATRON" [13]. The three-axis ACC signals were collected with a sampling frequency of 62.5 Hz. Additionally, an ECG was also measured as well, sampled at 250 Hz. The location of the accelerometer and the SENSATRON layout can be observed in Fig. 2.

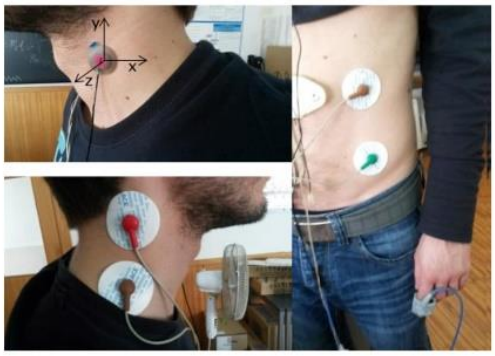

Fig. 2- Location of the accelerometer (top left). The ECG sensors of the SENSATRON (bottom left and right) (more details about the system can be found in [13]).

B. Implemented Algorithm for signal classification

The classifier algorithm based on a classical training and testing approach was developed using six different features. The implemented processing stages comprise two distinct phases. In the first pre-processing phase the extraction of the signal features is performed. In the second phase, a simple threshold-based classifier is applied, for which the optimal threshold was determined during the training phase based on a ROC analysis. The performance of the classifier is evaluated using the test-data set. Furthermore, feature relevance was assessed using the F-measure approach [14] in order evaluate features providing complementary information to be integrated into a multi-feature classifier.

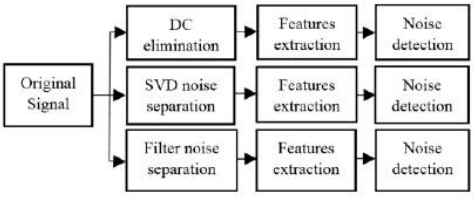

Fig. 3- Scheme of the different pre-processing steps.

1st Phase: in the first phase, each of the axis of the ACC signal was pre-processed for feature extraction using three different approaches depicted in Fig. 3. It was filtered with three different high-pass filters. In the simplest pre-processing stage, a 5th order Butterworth high-pass filter with cut-off frequency of 0.07 Hz was applied in order to eliminate the DC component. In the other two pre-processing stages the rational was to isolate the high-frequency noise content from the actual carotid pulse induced acceleration signal and to extract features from the former. This is based on the observation that movement artifacts tend to exhibit higher frequency components compared to the non-disturbed carotid signal.

In the filter-based noise separation approach, the cut-off frequencies were determined using a simulation modeling radius variation of the carotid artery given a typical blood pressure of SBP = 120 mmHg and SBP = 80mmHg. A maximum expected heart rate for a person at rest, i.e., 80 bpm, and during resuscitation, i.e., 240 bpm. The pulse pressure wave was simulated using the model reported in [10]. Basic blocks of the simulation model are depicted in Fig. 4.

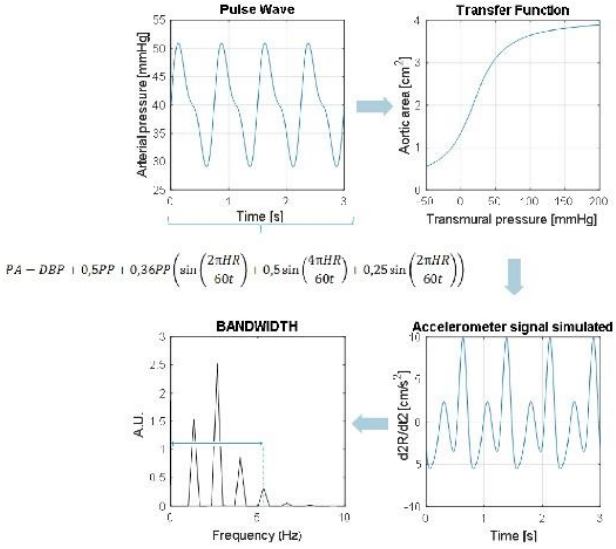

Fig. 4- Scheme of the simulation model. PA-arterial pressure; DBP-diastolic blood pressure; PP-pulse pressure; HR-Hear rate; t-instant of the pulse.

Using this approach, the actual cut-off frequencies were determined as 5.4 Hz and 16.0 Hz given that these frequencies correspond to the expected accelerometer signal bandwidth at 80 bpm and 240 bpm, respectively.

In the second noise separation approach the Single Value Decomposition (SVD) method is applied in order to identify signal components related to noise. Let $A \equiv (x_x, x_y, x_z) \in \mathbb{R}^{nx3}$, n - number of samples, be the matrix formed by appending the three axis of the accelerometer signal. The noise is separated by zeroing the two main singular values in matrix $\boldsymbol{S}$, **i.e.,**

$$\boldsymbol{A = USV^T} \quad (1)$$

In a next step, from these pre-processed signals the features were extracted as defined in equations (2)-(6), which are energy mean, variance of the energy, Shannon energy, third and fourth statistical moments to assess peakness and skewness of the signal distribution, and Teager energy). These

features were calculated using a 1.5 seconds centered moving window. All the features were normalized, by the mean of the signal amplitude acquired during the first lying down phase of the protocol.

$$E_{\mu} = \frac{1}{N_s}\sum x(n)^2 \quad (2)$$

$$E_{\sigma^2} = \frac{1}{N_s}\sum \left(x(n)^2 - E_{\mu}(n)\right)^2 \quad (3)$$

$$E_{sh} = \sum\left[x(n)^2 log\left(x(n)^2\right)\right] \quad (4)$$

$$Statistical\ Moment = \sum \frac{x(n)^t}{N_s} \quad (5)$$

$$E_{teager} = \frac{1}{N_s}\sum \left(x(n)^2 - x(n-1)x(n+1)\right) \quad (6)$$

x represents the signal, n represents the sample index; t represents the order of the moment (3 or 4); N_s = number of samples on the moving window.

2nd Phase: in this phase, the threshold-based classifier was tuned using a training dataset to estimate the optimal threshold using a ROC-approach. Performance was evaluated using an independent test dataset. The signals collected from the volunteers were randomly divided into these two groups to form the aforementioned datasets, i.e., the *training* dataset was defined using the data collected from two thirds of the available individuals (8 subjects randomly selected), whereas the *test* dataset was constituted by the signals collected from the remaining individuals (4 subjects).

As was already mentioned, a ROC-based approach was applied using the training dataset in order to obtain the optimal threshold for each feature, i.e., the selected threshold value is the one that optimizes the tradeoff between sensitivity and specificity (see Fig. 5). It should be noted that, in order to avoid influence of uncertainty during the prolonged transitions between adjacent phases in the protocol (e.g. due to slow reaction of the subject), the first and last 2 seconds of each phase have not been considered for classification performance assessment. Another important point to mention is that the ground truth of the signals was defined by manual classification according to the different phases of the protocol. This could contribute to a decreased performance of the classifier.

Finally, there was the ranking of the most convenient features for the classifier, based on a score metric FSS, well explained in [14].

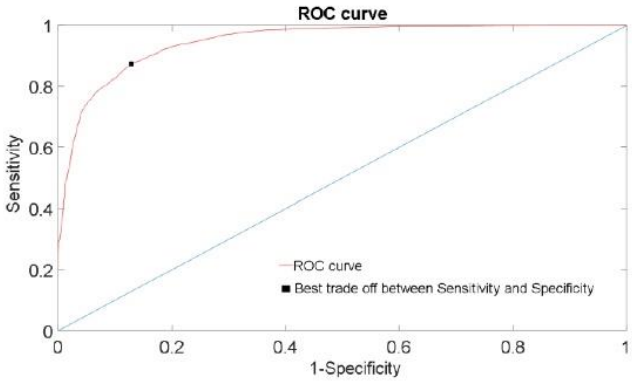

Fig. 5- Example of a ROC curve, and the point associated to the best balance between Sensitivity and Specificity.

III. RESULTS AND DISCUSSION

A. *Implemented Algorithm for signal classification*

Table 1 shows the best performance results to discriminate motion / no motion achieved using each of the individual accelerometer axis, the absolute value of the acceleration vector and the classification approach outlined in the previous section.

Axis	Accx	Accy	Accz	Abs. Acc
Sensitivity (%)	82.3	76.18	91.09	91.46
Specificity (%)	93.4	93.4	91.29	90.44

Table. 1- The best performance for the three different axis and the absolute value of acceleration.

According to table 1, the component that provides the best performance for the classifier was the component on the direction z (perpendicular to the skin- see Fig. 2), also very similar results are achieved using the absolute Acc value. In the following, only the results related to the z axis Acc and the absolute Acc value will be presented and discussed.

Table 2, summarizes the classification results in the test dataset achieved using the aforementioned noise detection approach for the various pre-processing configurations and derived features. For most of the features, the pre-processing that leads to the best results were the one derived with a high-pass filter

Pre-Processing Type\ Feature			Energy Mean		Energy Variance		3º Statistical Moment		4º Statistical Moment		Shannon Energy		Teager Energy	
			SEN (%)	SPE (%)	SEN (%)	SPE (%)	SEN (%)	SPE (%)	SEN (%)	SPE (%)	SEN (%)	SPE (%)	SEN (%)	SPE (%)
DC-Filter		Acc z	39.17	89.64	56	91.67	42.44	87.23	44.25	90.36	44.97	90.23	84.73	93.26
		Abs. Acc	66.18	81.55	64.27	88.15	59.43	76.63	69.36	74.55	69.55	73.93	85.67	93.11
SVD		Acc z	62.28	95.61	62.65	93.91	63.62	91.73	62.9	94.05	61.94	94.13	58.89	94.38
		Abs. Acc	81.03	90.36	59.91	93.2	67.59	91.15	60.78	91.95	60.32	93.08	69.67	93.39
Noise-Filter	fc=5.4 Hz	Acc z	**91.09**	**91.29**	73.74	91.88	74.84	86.45	78.1	91.62	77.52	91.64	88.8	91.54
		Abs. Acc	**91.46**	**90.44**	85.59	91.49	70.9	89.48	86.23	92.06	86.2	92.06	88.84	90.49
	fc=16 Hz	Acc z	74.48	89.11	70.12	87.59	71.13	74.66	72.37	86.79	73.98	84.88	74.46	88.87
		Abs. Acc	77.3	87.68	75.91	83.35	76.31	65.79	74.26	85.83	71.03	87.94	77.36	88.99

Table. 2- Classifier performance for all features, for the axis z selected and for the absolute value of the acceleration.

(fc=5.4 Hz or fc=16 Hz). Still, significant differences of the performance between the two cut-off frequencies can be

observed. These discrepancies might be caused by the fact that we acquired data from healthy people only doing regular and low-intensity exercises, therefore, the heart rate was usually below 80 bpm. We found very similar results for the best feature, i.e., SEN=91.09%, SPE= 91,29% using the z-axis and SEN=91.46%, SPE=90.44% using the absolute Acc value.

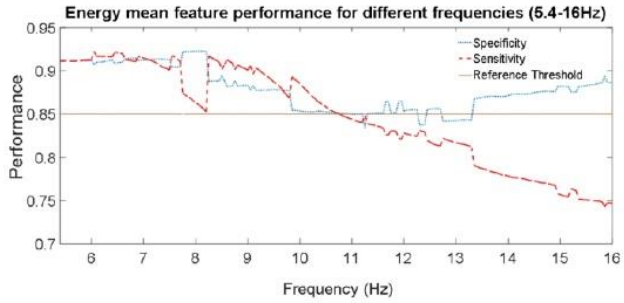

Fig. 6- Performance of Energy mean feature for different frequencies from 5.4 Hz to 16 Hz.

From table 2, it is also observed that the best approach for noise detection depends on the noise-filtering corner frequencies, i.e., extracting features after discarding the expected physiological frequency components of interest e.g. in our case heart rate. It is found that the simple energy mean feature exhibits the best performance and tends to provide stable results for a significant range of cut-off frequencies, with sensitivity and specificity values above 85 % until frequencies around 10.5 Hz (see Fig. 6). A similar observation was found for Teager energy. This feature exhibits good performance even when no noise filtering is applied, maybe due to the fact, that this feature is sensitive to both intensity as well as frequency of the signal.

Feature	Score (%)	AUC
Mean Energy	94.78	94.78
3º Statistical Moment	75.16	81.83
Teager Energy	40.77	94.11
4ºStatistical Moment	18.42	86.44
Energy Variance	10.17	85.71
Shannon Energy	-0.0227	78.4

Table. 3- Feature selection rank, of the axis z, according to the FSS measure.

In table 3 we assess the level of feature relevance using the FSS measure approach for the selected components. The FSS measure combines the classification performance (using the area under curve – AUC - of the ROC) and the level the feature's independence with respect to other relevant features (average Spearman's correlation with respect to other relevant features). Although the Teager Energy exhibits a similar AUC value compared to the average energy, it is ranked in a lower position compared to the third statistical moment, due to its higher correlation with respect to the energy mean. Furthermore, only the energy mean and the third statistical moment feature exhibit a F-score higher than 50%. This suggests that the remaining assessed features do not contribute with relevant added information to describe the problem's domain. Therefore, they might be irrelevant if more complex multi-feature classifier are to be designed for artifact detection in Acc signals measured at the carotid.

IV. CONCLUSION AND FUTURE WORK

In this paper we investigate the application of low computational complexity features in the detection of movement artifact in accelerometer signals acquired from the carotid. Using a dataset collected from healthy subjects, we have shown that the first and the third statistical moments of the signal's energy seem to be sufficient to adequately detect artifacts induced by expected activities, both intensive movements as well as at rest. Our simple approach seems promising, still, it needs to be confirmed with data collected in representative populations of intended core applications. Other directions for future work comprise (1) the assessment of the ACC signal quality in terms of diagnostic value during artifact contamination and (2) to explore disturbance of the quasi-periodic nature of pressure pulses in order to detect artifacts.

REFERENCES

[1] C. D. Deakin, et.al. Accuracy of the advanced trauma life support guidelines for predicting systolic blood pressure using carotid, femoral, and radial pulses: Observational study. BMJ 2000, vol. 321 673-674

[2] S. Brearley, et.al. Peripheral pulse palpation: an unreliable physical sign," Annals of The Royal College of Surgeons of England, vol. 74, pp. 169–171, 1992.

[3] M. Lundin, et.al. , "Distal pulse palpation: is it of Surgery, vol. 23, pp. 252-255, 1999.

[4] Eberle, W. et.al. , "Checking the carotid pulse check: diagnostic accuracy of first responders in patients with and without a pulse," Resuscitation, vol. 33, pp. 107-116, 1996.

[5] [6] F. J. Ochoa, et.al. , "Competence of health professionals to check the carotid pulse," Resuscitation, vol. 37, pp. 173-175, 1998.

[6] Tăuţan AM, et.al., Characterization and reduction of motion artifacts in photoplethysmographic signals from a wrist-worn device. Conf Proc IEEE Eng Med Biol Soc. 2015;2015:6146-9

[7] Wijshoff RW, et.al. Reduction of Periodic Motion Artifacts in Photoplethysmography. IEEE Trans Biomed Eng. 2017 Jan;64(1):196-207.

[8] Robert Mooney, et.al. Inertial Sensor Technology for Elite Swimming Performance Analysis: A Systematic Review, Sensors 2016, 16, 18

[9] L. Schmitt, J. Muehlsteff J, "Patient monitoring on general wards – Needs, challenges and opportunities for monitoring respiration rate," Biomed Tech (Berl). 60(S1):67, 2015

[10] J. Muehlsteff, K. Dellimore, V. Aarts, et al., "Feasibility of pulse presence and pulse strength assessment during head-up tilt table testing using an accelerometer located at the carotid artery," Conf Proc IEEE Eng Med Biol Soc., pp. 894-897, 2014.

[11] J. Muehlsteff, K. Dellimore, V. Aarts, et al., "Pulse detection with a single accelerometer placed at the carotid artery: Performance in a real-life diagnostic test in fainting patients," Conf Proc IEEE Eng Med Biol Soc., pp. 434-437, 2015.

[12] K. Dellimore, R. Wijshoff, C. Haarburger, et al., "Towards an algorithm for automatic accelerometer-based pulse presence detection during cardiopulmonary resuscitation," Conf Proc IEEE Eng Med Biol Soc., pp. 3531-3534, 2016.

[13] J. Muehlsteff, P. Carvalho, J. Henriques, et al., "Cardiac status assessment with a multi-signal device for improved home-based congestive heart failure management," Conf Proc IEEE Eng Med Biol Soc. 2011, pp. 876-879.

[14] R. Couceiro, P. Carvalho, R. P. Paiva, J. Muehlsteff, J. Henriques, C. Eickholt, C. Brinkmeyer, M. Kelm, and C. Meyer, "Real-Time Prediction of Neurally Mediated Syncope", IEEE Journal of Biomedical and Health Informatics, vol. 20, no. 2, March 2016.

Appendix B

“Robust Carotid Pulse Detection Using Accelerometry and Electrocardiography”,

Scientific publication submitted and accepted to be presented at the 3rd International Forum on Research and Technologies for Society Industry (RSTI 2017) of the Institute for Electrical and Electronics Engineers (IEEE), in Modena, Italy, 2017. Authors: B. Silva, J. Muehlsteff, R. Couceiro, J. Henriques, C. Peiker, C. Meyer and P. Carvalho.

Robust Carotid Pulse Detection Using Accelerometry and Electrocardiography

B. Silva, J. Muehlsteff, R. Couceiro, J. Henriques, C. Peiker, C. Meyer, P. Carvalho

***Abstract* — Neurally mediated syncope (NMS) is a disorder of the autonomic regulation of postural tone. These patients suffer from blood-pressure regulation failure resulting in hypo-perfusion of the brain, which might lead to significant injuries due to falls. Detection of the onset of blood-pressure regulation failure enables the patient to start counter-measures and, hence, avoid hypo-perfusion of the brain. Monitoring of blood-pressure (BP) changes is key to develop an early alert solution. Several setups have been tested for this purpose using vascular unloading and pulse arrival time (PAT).**

The aim of this study was to do an initial investigation of using the electrocardiography (ECG) signal and accelerometry (ACC) signals acquired from the carotid to reliably infer pulse presence and pulse absence. A classifier using a correlation feature derived from the ECG and the ACC signals was conceptualized and implemented. The algorithm performance was tested with data acquired during scheduled head-up tilt table tests of 8 syncope patients. This is an essential step towards PAT inference as a BP surrogate.

I. INTRODUCTION

Neurally mediated syncope (NMS) is one of the twenty most important reasons for emergency department (ED) admissions in Germany [1]. It is a disorder of the autonomic regulation of postural tone [2]. NMS patients suffer from hypotension and/or bradycardia, which result in cerebral hypo-perfusion. This can finally lead to a sudden, transient loss of consciousness with spontaneous recovery [2]. NMS is associated with a higher risk of falls, which is in particular a problem in the elderly. It compromises quality of life, is one of the root causes for injuries due to falls and therefore causes financial costs to the healthcare system [2-4]. Effective early warning systems for the management of high risk populations, which are able to predict an impending NMS event via the assessment of pulse strength (PS) and by monitoring trends in surrogate blood pressure parameters, is a highly relevant and interesting area for innovations. For this purpose, accelerometry (ACC) sensors might offer a promising sensing modality, since low cost, low power, small and inexpensive ACC sensors with high sensitivities are available. We have demonstrated in our previous work the basic feasibility of ACC-based pulse detection from signals acquired from the carotid artery [5-6]. We also developed an algorithm to deal with motion artifacts more satisfactorily [7]. Preferably a single ACC sensor would be able to detect impending NMS events. However, we found that ACC-based pulse detection is compromised by arrhythmia or artifacts due to, e.g., talking and head movements [5]. Therefore, we investigated the combination of ACC and electrocardiography (ECG).

The aim of this study was to perform a first initial investigation of a signal fusion concept to improve our previous results. It is based on fusing ECG and ACC signals inspired by calculating a cross-correlation feature for discrimination of pulse presences / absence as described in [8]. Additionally, we included the motion artifact classifier as discussed in [7].

II. METHODS

A. Experimental Protocol and Setup

The data collection study was performed using the investigational device "Sensatron" from Philips [5]. This bio-signal acquisition platform enables the synchronous measurement of ECG signals and multiple three-axis ACC signals. In our experiments, one of the ACC sensors has been positioned on the carotid (see Fig. 1).

The three-axis ACC signals were sampled at 125 Hz, and the ECG signal at 250 Hz. Since we are interested in the artery dilation signal, which appears mostly in the ACC z-axis [7], we have analyzed this signal only.

Our analysis is based on a subset of data gathered during scheduled head-up tilt table tests (HUTT) involving 27 patients with an unexplained history of syncope [5].

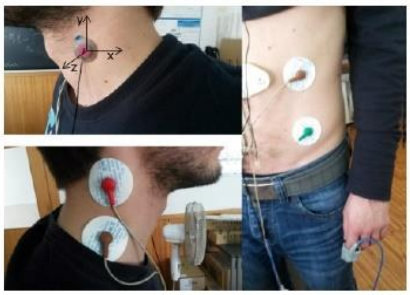

Fig. 1- Top left: location of the accelerometer. Bottom left and right: ECG sensors of the Sensatron. Image adapted from [7].

This work was supported by project LINK (H2020 – 692023). B. Silva, J. Henriques and P. Carvalho are with CISUC, Department of Informatics Engineering, University of Coimbra, Portugal (e-mail: bernardosilva1694@gmail.com, {rcouceir, jh, carvalho,} @dei.uc.pt).
J. Muehlsteff is with Philips Research, Eindhoven, The Netherlands (email: jens.muehlsteff@philips.com). Christiane Peiker and Christian Meyer are with UKE Eppendorf University Hospital Hamburg, Division of Cardiology, Pneumology, and Angiology, e-mail: chr.meyer@uke.de.

Date of 8 patients 5 male and 3 female with an average age of (56 ± 23) years and a BMI of (26.5 ± 5.6) kg.m^{-2} were used in this work. These patients had different cardio-vascular conditions such as arrhythmias or structural heart diseases.

Since HUTT data typically does not include well-defined phases without pulse information, we also acquired ACC signals without pulse information artificially in lab tests. This data set was collected using the ACC sensor of the "Sensatron" device by (i) attaching the sensor on the back of a hand to simulate a no / low pulse signal, and (ii) placing the ACC sensor on a table (sensor is not attached at all). These segments representing "Pulse absence" were placed randomly in the HUTT data. Only the original ACC signals were replaced. Each "Pulse absent" phase has a duration of 5 minutes, in which any external disturbance was avoided. One signal stream generated by this procedure is shown in Fig. 2.

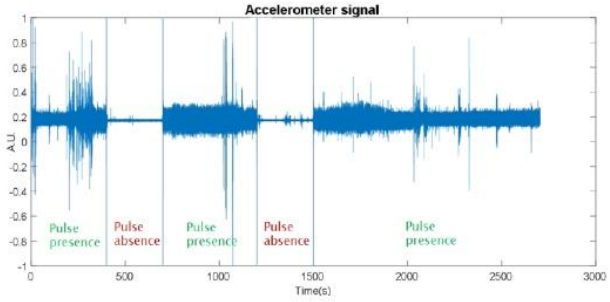

Fig. 2- Representation of a generated ACC signal (patient 1); segments between the blue vertical lines represent phases with (green label) or without (red label) pulse.

One patient exhibited severe atrial fibrillation resulting in ACC signals of low signal-to-noise (SNR). The ECG of one patient was considerably contaminated with power line noise and another one contained Premature Ventricular Contractions (PVCs) as shown in Fig. 3. These issues could affect the performance of the algorithm but also illustrate the broad range of situations that the method will face and should be able to handle in a real-life application.

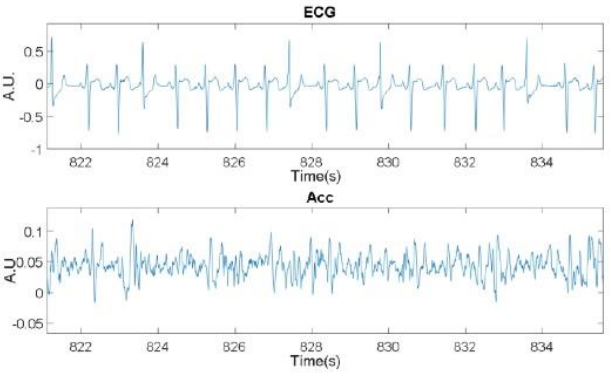

Fig. 3- Premature Ventricular Contractions in Patient 8.

B. Implemented algorithm for pulse presence detection

The proposed method for pulse detection is depicted in Fig. 4. The main idea of the algorithm is to explore a signal fusion concept of the ACC and ECG signals. The first stage of the algorithm identifies noise due to body movement, speaking and head movement using the method as reported in [7]. Our noise detection method is tuned for the presence of high-frequency or high intensity interferences in the carotid ACC signal. In the second processing stage a correlation feature from pre-processed ECG and ACC signals is derived for sliding windows [8]. Finally, in phase three, a simple threshold-based classifier is applied to detect pulses. The optimal threshold was identified using an ROC approach on the *training* data.

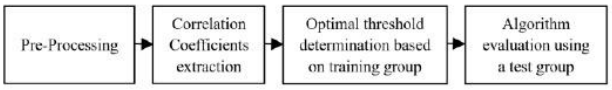

Fig. 4- Main stages of the proposed algorithm.

These phases are described in detail below:

1st Stage: This stage prepares the ECG and ACC signals for the correlation assessment. For this purpose, the ECG signal was resampled at 125 Hz to have the same sampling frequency as the ACC signal. Subsequently a 5th order Butterworth high-pass filter with a cut-off frequency of 0.5 Hz was applied in order to eliminate baseline noise. In a next step, two parallel procedures were implemented for the ACC signal: (i) the signal was high-pass filtered (details below) and (ii) the noise in the ACC signals was detected per sample and annotated in order to avoid further processing. The percentage of signal contamination for each patient was calculated according to (1).

$$Contamination\ (\%) = \frac{\text{total number of contaminated samples}}{\text{total number of samples}} \times 100 \quad (1)$$

The ACC signal was high-pass filtered using a 5th order Butterworth filter with a cut-off frequency higher than 0.5 Hz to eliminate the DC component as well as any type of low-frequency contamination such as muscle movements and vasomotion. Furthermore, an increase in the cut-off frequency highlighted the main peaks in the ACC signal, which were due to the carotid pulse and, therefore, improved the correlation with the ECG signal (see Fig. 5). After this phase, the noise-contaminated sections of the ACC signal were identified, having little or no influence, for further processing. To assess the optimal cut-off frequency for the high-pass filter applied to the ACC signal, an ROC analysis was performed using a test set, as it is illustrated in Fig. 6. We found as an optimal cut-off frequency fc=5 Hz. For each cut-off frequency we defined an optimal threshold for the classifier using an ROC approach.

2nd Stage: In this stage, the correlation between the ACC and ECG was determined using a sliding 3 seconds window with 75% of overlap. From each window, the absolute maximum of the normalized correlation coefficients was extracted for further assessment of pulse presence. In order to reduce noise interference, correlation was only assessed if the percentage of uncontaminated samples in the analysed window was below a pre-defined threshold L. After a careful and detailed analysis, it was observed that changes on the percentage L of contamination had only minor influence on the performance of the algorithm and we fixed L to 20%. To minimize loss of samples, contiguous contaminated sections with less or with 10 samples, were reconstructed using linear

interpolation. For contiguous sections of contaminated ACC signals greater than 10 samples, the affected samples and their ECG counterparts were removed from further processing. Fig. 7 presents the correlation coefficients for two patients using the pre-processing steps discussed before.

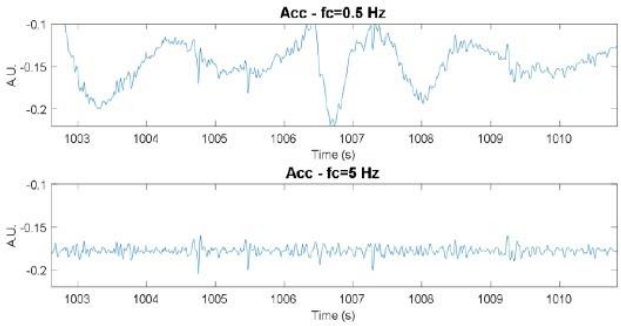

Fig. 5- ACC signal after a high-pass filter has been applied. Upper diagram: a high-pass filter with a cut-off frequency of 0.5 Hz; lower diagram: a high-pass filter with a cut-off frequency 5 Hz.

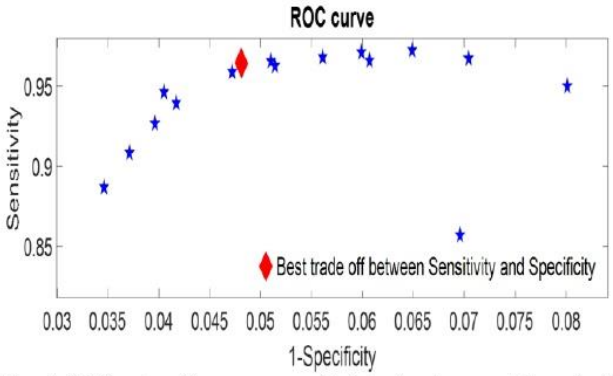

Fig. 6- Different performances associated to the change of the cut-off frequency.

	Contamination level
patient 1	6.67%
patient 2	15.75%
patient 3	6.52%
patient 4	3.59%
patient 5	37.09%
patient 6	8.50%
patient 7	44.83%
patient 8	7.83%

Table. I- Level of contamination identified on the ACC signal by the noise classifier for each patient.

3rd Stage: In this stage, using an ROC-based approach, the optimal threshold was determined for a *training* dataset, i.e., the threshold that optimized the trade-off between sensitivity and specificity (see Fig. 8) [7] and then evaluated using an independent *test* dataset. The *training* and the *test* dataset were defined randomly at the patient level, i.e., two thirds of the patients in the database (5 subjects) were selected as part of the *training* group, and the remaining 3 patients formed the *test* group. The ground truth of these signals was defined by manual annotation.

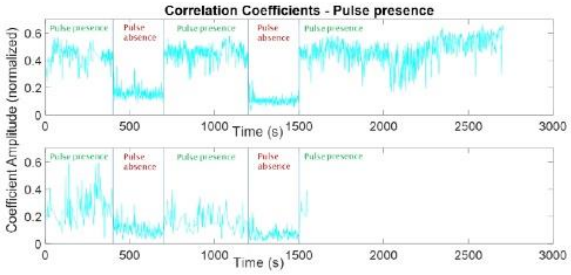

Fig. 7- Correlation coefficients extracted from the entire signal for two patients. Segments between the blue vertical lines represent the inserted "pulse absence" segments (Patient 1 - upper panel; Patient 5 - bottom panel; fc=5Hz; L=20%).

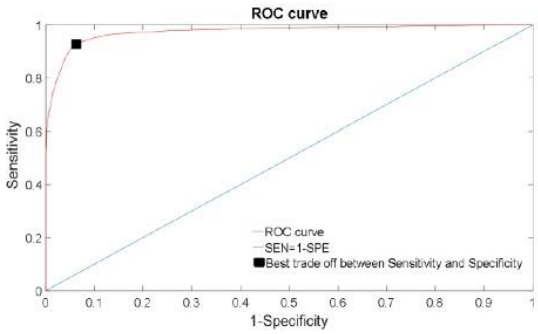

Fig. 8- Example of an ROC curve, and the point associated to the best balance between Sensitivity and Specificity.

III. RESULTS AND DISCUSSION

A. Implemented algorithm for pulse presence classification

Table. I shows the level of the ACC artefacts of each patient as identified by the noise classifier. As can be observed, the level of contamination was relatively small for most of the patients, but not for patients 5 and 7. A large portion of the acquired signals was lost.

In Table II it is presented the results per patient using the best threshold to identify possible outliers, as well as to verify if the performance of the algorithm in the referenced patients (2, 5 and 8) has been affected. For patient 2 and patient 5 the achieved sensitivity values were lower compared to the results for the other patients. The sensitivity for patient 5 is even lower than patient 2.

Patient	1	2	3	4	5	6	7	8
SEN(%)	99.55	86.08	98.25	98.61	60.78	94.82	99.38	92.26
SPE(%)	95.07	92.41	94.3	89.49	97.97	95.2	93.81	95.82

Table. II- Sensitivity and specificity for each patient when the optimal threshold was used.

Table. III summarizes the average performance of our algorithm, evaluated with the test group, using the optimal threshold determined from the entire data set. We found very

good results, with SEN = 94.54% and SPE = 94.26% for this initial implementation.

	Test Group	Global
SEN(%)	96.58	94.54
SPE(%)	94.9	94.26

Table. III- Performance of the algorithm and Global (entire dataset-8 patients) results (fc=5Hz; L=20%).

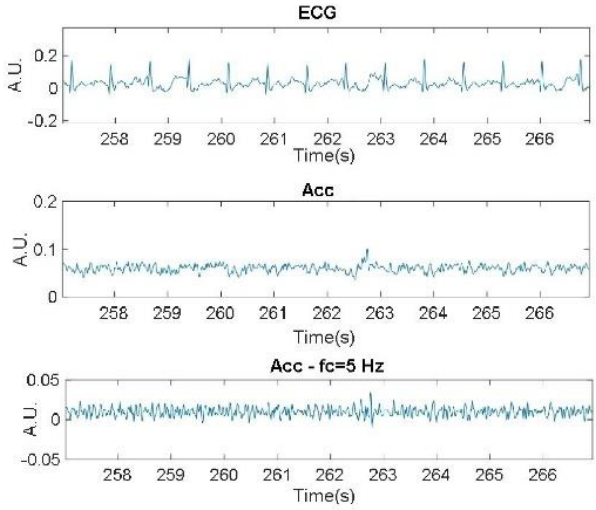

Fig. 9- Examples of Signals of Patient 5: (top) Filtered ECG; (middle) non-filtered ACC; (bottom) filtered ACC fc=5IIz.

The correlation coefficients of patient 5 shown in Fig. 7 (bottom) exhibit a low contrast for phases of pulse absence versus phases with pulse. Also, we observe large variations in the correlation coefficient, which might be caused by the powerline interference in the ECG, as well as a low SNR of the ACC signal, as can be observed in Fig. 9. This leads to a weak separation of pulse presence versus absence, being difficult to discriminate them solely using a simple thresholding approach. Hence a significant misclassification is obtained for patient 5.

For ACC signals with a high SNR making a pulse easily observable, the correlation coefficient seems very well determined and able to separate phases of pulse presence versus pulse absence reliably. This is illustrated in Fig. 7 (top) where periods without pulse have a correlation coefficient of lower than 0.2, and where phases with pulse typically have a higher correlation coefficient.

IV. CONCLUSION AND FUTURE WORK

In this paper we introduced a simple algorithm based on a signal fusion approach of synchronously acquired ECG and ACC signals to discriminate pulse presence / pulse absence. The proposed method is simple and can be easily implemented in devices with low processing power: a similarity metric based on a simple linear correlation coefficient seems to provide a reasonable feature for pulse presence detection after the ECG signal has been high-pass filtered. A simple threshold-based classifier is applied to discriminate pulse presence / absence. Although the presented results have been assessed on a small database, these initial results are promising, since we found consistent performance even for patients with severe arrhythmia. Next steps comprise to include more patients from the available database and to extract pulse arrival times using the ECG and the ACC signal as BP surrogate to infer an impeding syncope similar to our previously developed NMS algorithm based on a photoplethysmography signal.

REFERENCES

[1] https://www.destatis.de

[2] N. L. Rollinson, "Understanding and managing neurally nediated syncope in the adolescent," J Sch Nurs, 2005, v21(4):200-7.

[3] M. Anpalahan, "Neurally mediated syncope and unexplained or nonACCidental falls in the elderly," Intern Med J, 2006; 36(3):202-7.

[4] J. J. Seger. "Syncope Evaluation and Management," Tex Heart Inst J. 2005, vol. 32(2), pp. 204–206

[5] J. Muehlsteff, K. Dellimore, V. Aarts, et al., "Pulse detection with a single ACCelerometer placed at the carotid artery: Performance in a real-life diagnostic test in fainting patients," Conf Proc IEEE Eng Med Biol Soc., pp. 434-437, 2015.

[6] K. Dellimore, R. Wijshoff, C. Haarburger, et al., "Towards an algorithm for automatic ACCelerometer-based pulse presence detection during cardiopulmonary resuscitation," Conf Proc IEEE Eng Med Biol Soc., pp. 3531-3534, 2016.

[7] B.Silva, J. Muehlsteff, R.Couveiro, J. Henriques, P.Carvalho, "Artifact detection in ACCelerometer Signals acquired from the Carotid", Conf Proc IEEE Eng Med Biol Soc.2017. (ACCepted for presentation).

[8] Liang Wei, Tao Yu, Peng Gao, Weilun Quan, Yongqin Li, Detection of Spontaneous Pulse Using ACCeleration Signals Acquired From CPR Feedback Sensor in Porcine Model of Cardiac Arrest, Circulation, Volume 134, Issue Suppl 1